

Cost Effective Design of RC Building Frame Employing Unified Particle Swarm Optimization

Payel Chaudhuri (✉ payelce@gmail.com)

Indian Institute of Technology, Kharagpur <https://orcid.org/0000-0003-2214-9554>

Swarup Barman

Indian Institute of Technology Kharagpur

Damodar Maity

Indian Institute of Technology Kharagpur

Dipak Kumar Maiti

Indian Institute of Technology Kharagpur

Research Article

Keywords: cost effective design, unified particle swarm optimization, STAAD Pro, RC building frame, wind load, seismic load.

Posted Date: April 28th, 2021

DOI: <https://doi.org/10.21203/rs.3.rs-227713/v1>

License: © ⓘ This work is licensed under a Creative Commons Attribution 4.0 International License.

[Read Full License](#)

29 **Key words:** cost effective design, unified particle swarm optimization, STAAD Pro, RC
30 building frame, wind load, seismic load.

31 **1. Introduction**

32 Reinforced concrete is a dominant material for constructing various civil engineering
33 structures due to its high compressive strength, durability and resistance to damage from fire
34 and water. Conventional trial and error based design of RC structures is based on only safety
35 criteria, and requires excessive materials. Thus construction costs of building increases. So,
36 increase in use of reinforcement concrete comes with the demand for economical design.
37 Thus, from last few decades, researchers have proposed different method for cost
38 optimization of RC frames. Increase in computational power of computers has enhanced the
39 willfulness of such attempts drastically. Main challenge in optimizing the RC structures are
40 number of optimizing variables in comparison with the optimal design of steel structures,
41 where only material is considered for entire structures and cost of the entire structure is
42 proportional to weight of that material. On the other hand, cost of RC structures consist of
43 cost of concrete, cost of steel reinforcement and cost of formworks. Their unit costs differ
44 from each other. Their inter-relations are not simple, because any two of them change
45 significantly with slight changes in the quantity of the third factor. This in turn changes the
46 total cost of RC frame to a great extent. Thus, the actual problem comes to finding
47 appropriate combination of values for three aforementioned components of costs without
48 violating the safety requirements so that the total cost becomes minimum. Again, RC sections
49 are cast in situ. So, while designing cost effective sections, size of the sections and
50 reinforcement detailing should be provided to meet the specific demands from architectural
51 and construction point of view. Thus, presence of all these factors along with constraints
52 regarding strength, serviceability, architectural demands and easiness of construction make
53 cost optimization of real life RC structures a highly cumbersome task. However, in the same
54 time an algorithm to optimize the cost of a RC building frame satisfying all the necessary
55 criteria will be a valuable tool to the design practitioner.

56 Despite all these challenges many researchers have tried to find cost optimize designs of
57 RC building components. Milajić et al. [1] reviewed various methods available in literatures
58 for optimal design of reinforced concrete structure. They focused on the problems of these
59 existing methodologies, such as: gap between the theory and practice in the field, lack of
60 universal criteria and standard benchmark problem etc. Also, when ones talks about of cost

61 optimized design of a complete RC building project, it includes optimizing the topology of
62 the building, material costs of the building components, reinforcement distribution, cost of
63 shuttering, labor cost maintaining all the safety guidelines of competent authority.

64 Topology optimization of building means finding out optimum layout of the building for
65 a particular project. Topology optimization is a very popular and common term in steel
66 structures, where topology of truss is optimized to achieve cost optimum design [2].
67 However, researchers also tried to implement the concept of topology optimization also in
68 case of concrete structures by various means, such as windowed evolutionary structural
69 optimization (WESO) [3], plastic design layout optimization technique [4], dynamic
70 programming utilizing genetic algorithm (GA) based multi objective optimization [5]. Apart
71 from that, Zegard et al. [6] have implemented three different methods of topology design
72 optimization in building engineering. However, in real project topology is not decided solely
73 based on cost only. There are other deciding factors such as utility of the building, aesthetic
74 beauty or client's wish. Labor cost depends on the location of the construction and days
75 required to finish the construction. This can be managed with proper
76 construction management and planning strategies like Critical Path Method (CPM) and
77 Project Evaluation and Review Technique (PERT). Thus, present study is focused on the
78 optimizing the design of the structural components of a building frame.

79 Structural components, such as, beams, columns, slab and foundation contribute most in
80 the total cost of a project. Thus, cost optimum design of structural components are of utmost
81 importance for minimizing the project cost. Cost optimum design of RC beams have been
82 attempted by researchers utilizing various methods, simplex and Lagrangian optimization
83 method [7], geometric programming [8], GA based algorithm [9, 10], polynomial
84 optimization technique [11], simulated annealing [12], random search technique (RST) [13],
85 charged system search (CSS) [14]. Cost optimum design of T-beams [15] and cost optimum
86 design RC columns [7, 16, 17] also have been attempted. Apart from beam and column
87 optimization, design of reinforced concrete (RC) flat slabs have also been optimized by
88 Aldwaik and Adeli [18] using Neural dynamic model for Adeli and Park (NDAP) [19],
89 Design optimization of RC foundation has been performed by Chaudhuri and Maity [20].
90 Besides these individual structural components researchers have also tried to optimize the
91 beam-column frames in terms of weight [21], in terms of cost [22-29]. All these studies
92 regarding design optimization of RC building components or frames are conformed to the

93 guidelines decided by the various standards of different countries such as Indian standard (IS
94 456)[7,11, 20, 26], American standard (ACI 318, ASCE7)[13,17, 21-25, 28, 29], European
95 standard (Eurocode 2) [15,27]and Australian standard (AS 3600) [14], Brazilian standard
96 (NBR 6118)[12]. Apart from these, RazmaraShooli et al. [30] have proposed a GA-PSO
97 based algorithm for performance-based design optimization of a special moment-resisting
98 frames based on guidelines provided by American standards (ATC-40, FEMA 356, ASCE-7
99 and ASCE-41).In these literatures the researchers used geometry of beam, column, amount of
100 reinforcement, cost of material and shuttering as their optimization variable.In the problems
101 regarding optimized design of RC components, optimizing the distribution of reinforcement
102 are also an important issue [31, 32].

103 While solving any optimization problems choosing proper optimization techniques is
104 utmost important, every optimization techniques have their strengths and weaknesses. In this
105 regard, it is important to have an idea about the optimization techniques used by the
106 predecessors to solve a particular class of problems. The cost optimization design problems
107 of RC frames have been tackled by the researchers by using various optimization techniques.
108 Few of them have already been discussed earlier in this section. However, reviews of the
109 optimization algorithms used by researchers have been presented in Table 1 for clarity.

110 Thus, the key points, which have been observed from the above literature are as follows:

- 111 i) Literature studying the cost-optimum design of RC building are quite less in
112 number.
- 113 ii) Most of the literatures are focused on the optimization of only a particular
114 member (beam or column), and reinforcement detailing pattern of beam or column
115 sections.
- 116 iii) Also, no algorithm from above literature have been tested for large scale multi-
117 storey building frame to provide cost optimized design accompanied by
118 construction friendly reinforcement detailing.
- 119 iv) Usage of optimization techniques in this field is also very less compared to other
120 fields like structural health monitoring, travelling salesman problems, water
121 resource etc.

122 Apart from above points another important issue is the shortcomings of commercial
123 design software. Although, design performed in the software is correct in term of safety
124 criteria, they provide the reinforcement amount in terms area instead construction friendly
125 reinforcement detailing. Thus, the method developed in the present study aims towards
126 alleviate these shortcomings. Also Unified Particle Swarm Optimization has not been used
127 as a cost optimization method for multistory building design in the previous studies, although
128 it has been used very effectively in cost optimization of RC foundation [20], damage
129 detection problems [33-38], magnetoencephalography problem [39] etc. Hence, UPSO have
130 been found to be the appropriate optimization method for multistory building design and cost
131 optimization. Thus, main objective of the present paper is to develop cost-optimized design
132 algorithm for RC frames following the safety and serviceability requirements of IS 456 [40]
133 employing UPSO. Efficiency of the algorithm has been shown using two building frames
134 (G+8, and G+10) of different plan configurations. Effects of seismic and wind load also
135 have been considered. Optimization has been performed based on minimum cost rather than
136 minimum weight, as the considered building frames are not high-rise (Prakash et al. [7]).
137 Final optimized sections and reinforcement details obtained from the present algorithm can
138 be used without altering in the actual site during construction phase. The efficiency of the
139 developed design optimization algorithm has been investigated using Monte Carlo
140 simulation. Monte Carlo method estimates the probability of favorable solution of the
141 developed optimization algorithm when a large number of experiments are carried out for
142 cost optimization of both the buildings. This consequently evaluates the robustness of the
143 developed algorithm in case of huge number of experiments and different types of buildings.

144 **2. Mathematical formulation**

145 An UPSO based algorithm has been developed in the present study to obtain cost
146 effective design of the multi-storeyed reinforcement concrete frame. Details of structural
147 analysis, design criteria, optimization algorithm, objective functions have been discussed in a
148 brief manner in this section.

149 **2.1. Structural analysis**

150 In general building frames are subjected to gravity load (dead load (DL) and live load
151 (LL)), wind load (WL) and seismic load (SL). Designers use all these loads in various
152 combinations to calculate design forces such as axial loads, bending moments and shear

153 forces for beams and columns. The moments, shear forces and axial loads for the critical load
154 combination are used to design the beams and columns of the building frames. Detail
155 procedure for analysis of building frames under aforementioned loads is mentioned briefly in
156 the subsequent sections.

157 *2.1.1. Gravity loads*

158 Gravity loads consist of dead load and live load. Dead load of different components of a
159 building can be considered as per IS 875 (Part I) [41]. Dead loads constitute of the following
160 loads.

- 161 1. Self-weight of beams and columns.
- 162 2. Self-weight of internal and external wall and parapet wall.
- 163 3. Self-weight of floor slabs.
- 164 4. Dead load coming from floor finish and plastering

165 Any temporary or transient loads which act on the building can be defined as live loads.
166 People, furniture, vehicles, and almost everything else that can be moved throughout a
167 building come under live loads. Live loads can be provided to any structural element (floors,
168 columns, beams, even roofs). Appropriate amount and type of live load can be decided based
169 on the specification given on IS 875 (Part II) [42].

170 *2.1.2. Wind loads*

171 Wind load should be considered for designing a multi-storey building frame. The nature
172 of flow of wind past a body resting on a surface depends on the conditions of the surface, the
173 shape of the body, its height, velocity of wind flow and many other factors [43]. IS 875 (Part
174 III) [44] contains the guidelines for considering the effects of wind on a multistorey building.
175 The shape of wind load velocity profile is similar to boundary layer flow profile. A typical
176 velocity profile of wind load considered for analysis has been shown in Fig. 1. The dotted
177 line represents boundary layer. In general velocity is zero at the ground and increases up to
178 the boundary layer. Beyond boundary layer wind velocity does not change with height. As
179 the wind travel in upstream direction through a particular terrain, the wind profile changes
180 and velocity and height of boundary layer increases. The distance travelled by a wind profile

181 on a particular terrain is called fetch length, i.e. x_1 and x_2 in Fig. 1. Upward penetration of the
 182 velocity profile at any fetch length is called developed height, i.e., h_1 and h_2 in
 183 Fig.1. Developed height increases up to gradient height, where velocity become maximum.
 184 After that even if wind travel upstream direction velocity profile remain unchanged. At this
 185 point it can said that velocity profile is fully developed for that particular terrain. In case of
 186 wind analysis of a structures generally it is assumed that wind profile is fully developed
 187 before hitting the structure. The values of a fully developed velocity profile depends on the
 188 terrain category. As the terrain category becomes rougher, gradient height increases. IS 875
 189 (Part III) [44] have provided the multiplier for velocity profile for each terrain category.

190 Initially wind analysis of any structure starts with selecting proper basic wind speed V_b
 191 depending on the location of the structure. The design wind speed V_z at height z in m/s can be
 192 calculated mathematically as per Eq. 1.

$$V_z = V_b k_1 k_2 k_3 k_4 \quad (1)$$

193 Here, k_1 is risk factor or probability factor. It is decided based on design life of structures.
 194 k_2 is the velocity profile multiplier based on the terrain category. k_3 is topography factor,
 195 decided based on the ground slope of the site. k_4 is a factor based on the cyclonic importance
 196 of the structure.

197 The wind pressure in N/m^2 at any height z above the mean ground level can be obtained
 198 from the following Eq. 2.

$$p_z = 0.6 V_z^2 \quad (2)$$

199 Finally design wind pressure (p_d) in N/m^2 at any height z above the mean ground level
 200 can be obtained from the following Eq. 3.

$$p_d = K_d K_a K_c p_z, p_d \geq 0.7 p_z \quad (3)$$

201 Design moment, shear and axial forces in beams and columns for wind load are calculated by
 202 applying the design wind pressure on the frame.

203 *2.1.3. Seismic loads*

204 When, any structure is subjected to seismic load dynamic equation of the structure can be
205 represented as Eq. 4.

$$[M]\ddot{x}(t) + [C]\dot{x}(t) + [K]x(t) = -[M]\ddot{u}_g(t) \quad (4)$$

206 Where, $[M]$, $[C]$ and $[K]$ are mass, damping and stiffness matrix of the structure. $\ddot{u}_g(t)$ is the
207 acceleration time history of the induced earthquake. $x(t)$ is the time history response of the
208 structure due to the induced earthquake force. Equation 4 can be solved using numerical
209 approaches for time history responses, such as displacement $x(t)$, velocity $\dot{x}(t)$ and
210 acceleration $\ddot{x}(t)$. Eventually stress time history also can be obtained. But, there are some
211 difficulties to do an actual seismic analysis for every structure to be designed. They are

212 i) It is not always possible to have the earthquake acceleration time history of the
213 exact location of the structure.

214 ii) Analysis of the structure cannot be carried out solely considering the peak ground
215 acceleration (PGA) of the earthquake, as the response of the structure depends on
216 the frequency component of the earthquake and its own dynamic properties.

217 These difficulties can be overcome by using the response spectrum of the earthquake instead
218 of using the acceleration time history as input. Response spectrum represents the maximum
219 response of damped single degree of freedom (SDOF) system for a particular input
220 earthquake motion at different natural period. Maximum response is more important to a
221 designer than the entire time history. One can also obtain mean response spectrum for a
222 particular location using more than one data of past earthquakes of the location. Also, use of
223 different damping value will give different response spectrum for same earthquake response.
224 Once acceleration response spectrum is known, one can easily obtain the maximum base
225 shear simply by multiplying the spectral acceleration obtained from the response spectrum
226 with the seismic mass of the structure. Every country develops their own design response
227 spectrum based on the past earthquake happenings in the region. In general seismic design
228 practice the structure should prevent non-structural damage for minor earthquake, prevent
229 structural damage with minimum non-structural damage for moderate earthquake and avoid
230 collapse to save lives in case of a major earthquake. Thus, no one use the spectral
231 acceleration associated with PGA (maximum considered earthquake (MCE)) for seismic

232 design of structure. Rather, the analysis is carried out for a much reduced value of spectral
233 acceleration (design basis earthquake (DBE)).

234 The guidelines for analyzing a building frame for seismic loading is mentioned in IS
235 1893(Part-I)[45]. Instead of solving rigorous dynamic equations, Indian standard has
236 provided simple linear static approach for simple regular structures utilizing the response
237 spectrum. Entire country has been divided into four seismic zone (II, III, IV, V) based on the
238 PGA. Seismic forces has two horizontal and one vertical components. For simple regular
239 building frame vertical component is ignored. The design horizontal seismic coefficient (A_h)
240 can be calculated as Eq. 5.

$$A_h = \frac{\left(\frac{Z}{2}\right) \left(\frac{S_a}{g}\right)}{\left(\frac{R}{I}\right)} \quad (5)$$

241 Here, Z is seismic zone factor depend on the seismic zone of the location of the structures. In
242 the term $\left(\frac{Z}{2}\right)$, $\left(\frac{1}{2}\right)$ factor used to reduce the MCE to DBE. I is the importance factor, decided
243 based on the occupancy and use of the structure. R is the response reduction factor depends on
244 the ductility, redundancy and overstrength of the structure. A structure with good ductility
245 will have high value of R , i.e., that structure will be designed for low seismic force. $\left(\frac{S_a}{g}\right)$ is
246 normalize spectral acceleration coefficient, which can be calculated based on the natural
247 period of the structure and soil type from the design response spectrum presented in the
248 standard (Fig. 2).

249 The natural period of ordinary RC building can be calculated from Eq. 6.

$$T_a = \frac{0.09H_{bl}}{\sqrt{D_{bl}}} \quad (6)$$

250 Now, the base shear can be computed for the building as a whole from the following
251 equation (Eq. 7).

$$V_B = A_h W \quad (7)$$

252 where, W is the seismic weight of the building which is calculated by adding full dead load
253 and 25 percent of the liveload.

254 The base shear in Eq.7 is distributed at the center of mass of all the floor levels of the frame.
255 These forces are distributed to the individual lateral load resisting elements through structural
256 analysis considering floor diaphragm action.

257 *2.1.4. Load combinations*

258 All the above loads are considered for suitable load combinations according to IS 875
259 (Part V)[46] with appropriate load factors. The load combinations have been mentioned
260 below

261 1. $1.5(DL + LL)$

262 2. $1.5(DL \pm WL)$

263 3. $(0.9DL \pm 1.5WL)$

264 4. $1.5(DL \pm SL)$

265 5. $(0.9DL \pm 1.5SL)$

266 6. $1.2(DL + LL \pm WL)$

267 7. $1.2(DL + LL \pm SL)$

268 Among all these load combinations only most critical load combination has been used for
269 designing each beam and column of the building frames.

270 *2.2. Structural design*

271 Beams and columns of all the frames were designed adopting Limit State Method as per
272 the guidelines provided in the Indian Standard IS 456 [40] in the present study. The design
273 procedure has been described briefly in the following sections.

274 *2.2.1. Beam design*

275 The design of beam is carried out based on limit state of collapse in flexure considering
276 plane section normal to the axis remains plane after bending. Longitudinal reinforcements in

277 beams are provided to carry bending moments, whereas stirrups are provided to carry shear
 278 forces. Design bending moment (M_u) and shear forces (V_u) for all beam sections are obtained
 279 from the structural analysis. At first the beam is designed to carry design bending moment.
 280 The limiting moment of resistance of balanced singly reinforced beam section due to flexure
 281 can be calculated as per Eq. 8.

$$M_{u,lim} = 0.36 \frac{x_{u,max}}{d_e} \left(1 - 0.42 \frac{x_{u,max}}{d_e} \right) b d_e^2 f_{ck} \quad (8)$$

282 If $M_u \leq M_{u,lim}$, then the beam section is designed as singly reinforced section. The required
 283 area of tensile reinforcement can be calculated from equation Eq. 9.

$$M_u = 0.87 f_y A_{st} d_e \frac{x_{u,max}}{d_e} \left(1 - \frac{f_y A_{st}}{b d_e f_{ck}} \right), \quad A_{st} \geq 0.85 b d_e / f_y \quad (9)$$

284 If $M_u > M_{u,lim}$, then the beam is designed as doubly reinforced section. Area of tensile
 285 reinforcement (A_{st1}) required for $M_{u,lim}$ is calculated from equation Eq. 9. The area of
 286 compression reinforcement for the excess moment i.e. ($M_u - M_{u,lim}$) is obtained from Eq.
 287 10.

$$M_u - M_{u,lim} = f_{sc} A_{sc} (d_e - d') \quad (10)$$

288 where, f_{sc} = design stress in compression reinforcement and it is obtained from Table I
 289 (Appendix III) corresponding to a strain of $0.0035 \frac{(x_{u,max} - d')}{x_{u,max}}$, $\frac{x_{u,max}}{d_e} = 0.53, 0.48, 0.46$ for
 290 $f_y = 250, 415, 500$ respectively. The area of corresponding tensile reinforcement (A_{st2}) for
 291 the excess moment ($M_u - M_{u,lim}$) is calculated in Eq. 11.

$$A_{st2} = f_{sc} A_{sc} / 0.87 f_y \quad (11)$$

292 longitudinal reinforcement of beams are provided based on A_{st}, A_{st1}, A_{st2} . Next, the provide
 293 beam section is checked for design shear force. Nominal shear stress for beam section shall
 294 be obtained from the following Eq. 12.

$$\tau_v = V_u / b d_e \quad (12)$$

295 The design shear strength τ_c of concrete is calculated from IS 456 [40] or Appendix III for
 296 grade of concrete and percentage of total tensile reinforcement provided. If $\tau_v \leq \tau_c$, minimum
 297 shear reinforcement shall be provided as per in Eq. 13.

$$s_v = \min \left(\frac{0.87 f_y A_{sv}}{0.4b}, 3d_e, 300 \text{ mm} \right) \quad (13)$$

298 If $\tau_c < \tau_v < \tau_{cmax}$, The shear reinforcement should be designed to carry a shear force $V_{us} =$
 299 $V_u - \tau_c b d_e$. τ_{cmax} can be obtained from IS 456 depending on the strength of the concrete.
 300 (Table II, Appendix III) The spacing of the shear reinforcement shall be provided as obtained
 301 from the following equation. Eq. 14.

$$s_v = \min \left(\frac{0.87 f_y A_{sv} d_e}{V_{us}}, \frac{0.87 f_y A_{sv}}{0.4b}, 3d_e, 300 \text{ mm} \right) \quad (14)$$

302 Once the longitudinal reinforcement and shear reinforcement had been designed, the beam
 303 should be checked to be safe against the serviceability criteria of limit state method. Thus,
 304 maximum deflection of the beam should be within the limit provided by the design standard.
 305 The total deflection of beam is thus calculated as per Eq. 15.

$$a_{td} = a_s + a_{cs} + a_{cc} \quad (15)$$

306 where, a_s is calculated for the usual method for elastic deformation theory using short term
 307 elasticity modulus E_c and effective moment of inertia I_{eff} given in Eq. 16.

$$\frac{I_r}{1.2 - \frac{M_r z}{M d_e} \left(1 - \frac{x}{d_e}\right) \frac{b_w}{b}}, I_r < I_{eff} \quad I_{eff} = < I_{gr} \quad (16)$$

308 where, $M_r = f_{cr} I_{gr} / y_t$, a_{cs} is the deflection due to shrinkage and it is calculated according to
 309 the equation Eq. 17.

$$a_{cs} = f_3 \phi_{cs} l^2 \quad (17)$$

310 where, $\varphi_{cs} = f_4 \frac{\epsilon_{cs}}{D}$, where, f_3, f_4 are calculated from IS 456 [40] annex C-3.1. (Appendix
 311 III). $\epsilon_{cs}=0.0003.a_{cc}$ is the deflection due to creep for permanent loads and is defined in Eq.
 312 18.

$$a_{cc} = a_{i,cc} - a_i \quad (18)$$

313 where, $a_{i,cc}$ is the initial plus creep deflection due to permanent loads obtained using an
 314 elastic analysis with an effective modulus of elasticity ($E_{ce} = E_c/(1 + \theta)$).

315 2.2.2. Column design

316 The design of column is done based on the same assumption for limit state of collapse in
 317 flexure i.e. plane section normal to the axis remains plane after bending. All compression
 318 members should be designed for a minimum eccentricity of load in two principal direction.
 319 Minimum eccentricity in design of columns can be obtained from Eq. 19.

$$e_{min} = \min\left(\frac{l_c}{500} + \frac{D_c}{30}, 20 \text{ mm}\right) \quad (19)$$

320 All the column sections are designed considering combined effects of axial load and biaxial
 321 bending moments. Thus, minimum eccentricity should be checked for both x and y direction
 322 bending separately. If the column is subjected to axial load P_u , biaxial moments M_{ux} and
 323 M_{uy} , the column section thus designed should satisfy for interaction ratio given by Eq. 20.

$$\left(\frac{M_{ux}}{M_{ux1}}\right)^{\alpha_n} + \left(\frac{M_{uy}}{M_{uy1}}\right)^{\alpha_n} \leq 1.0 \quad (20)$$

324 α_n is the exponent component whose value depends on P_u/P_{uz} . $\alpha_n = 1$ for $P_u/P_{uz} \leq$
 325 0.2 . $\alpha_n = 2$ for $P_u/P_{uz} \geq 0.8$. Linear interpolation should be used for intermediate values.
 326 P_{uz} is calculated from Eq. 21.

$$P_{uz} = 0.45f_{ck} A_c + 0.75f_y A_{scc} \quad (21)$$

327 M_{ux1}, M_{uy1} are the maximum uniaxial moment carrying capacity of the column section
 328 combined with the axial load P_u respectively for about x and y direction. Now, while

329 considering any particular direction bending two different cases can emerge based on the
 330 position of the neutral axis as shown in Fig. 3.

331 Case 1: When the neutral axis lies within the column section (Fig. 3b), the axial load
 332 carrying capacity and moment carrying capacity of the section can be calculated from Eq. 22
 333 and Eq. 23 respectively.

$$P_{u1} = 0.36k f_{ck} b_c D_c + \sum_{i=1}^n \frac{p_i b_c D_c}{100} * (f_{si} - f_{ci}) \quad (22)$$

$$M_{u1} = 0.36k f_{ck} b_c D_c^2 (0.5 - 0.416k) + \sum_{i=1}^n \frac{p_i b_c D_c}{100} * (f_{si} - f_{ci}) y_i \quad (23)$$

334 where $k = x_u/D$;

335 Case 2: If neural axis lies outside the column section (Fig. 3c) the axial load carrying
 336 capacity and moment carrying capacity of the section can be calculated from Eq. 24 and Eq.
 337 25 respectively.

$$P_{u1} = C_1 f_{ck} b_c D_c + \sum_{i=1}^n \frac{p_i b_c D_c}{100} * (f_{si} - f_{ci}) \quad (24)$$

$$M_{u1} = C_1 f_{ck} b_c D_c (0.5 D_c - C_2 D_c) + \sum_{i=1}^n \frac{p_i b_c D_c}{100} * (f_{si} - f_{ci}) y_i \quad (25)$$

338 where, f_{ci} is stress in concrete at the level of i-th row of reinforcement and can be calculated
 339 from Fig. 3d. f_{si} is stress in the i-th row of reinforcement can be obtained from Table III
 340 (Appendix III). C_1 is stress co-efficient and $C_2 D$ is the distance of the centroid the concrete
 341 stress block (Fig. 3d) measured from the highly compressed edge. C_1 and C_2 can be obtained
 342 from Eq. 26 and Eq. 27 respectively.

$$C_1 = \frac{A_{str}}{f_{ck} D_c} \quad (26)$$

$$C_2 = M_c/A_{str} \quad (27)$$

343 A_{str} is the area of the stress block (Fig.3d), and can be calculated from the Eq. 28.

$$A_{str} = 0.446f_{ck}D_c * (1 - (\frac{4}{21})(\frac{4}{(7k-3)})^2) \quad (28)$$

344 M_c is the moment of the concrete stress block (Fig. 3d) about highly compressed edge is
345 obtained as per Eq. 29.

$$M_c = 0.446f_{ck}D_c * (0.5 * D_c) - (8/49) * g * D_c^2 \quad (29)$$

346 Where g is geometric properties of the parabola (Fig. 3d) obtained from Eq. 30.

$$g = (0.446f_{ck} * (\frac{4}{(7k-3)})^2) \quad (30)$$

347 Diameter of tie bar of a column section (φ_{tie}) should be decided according to Eq. 31.

$$\varphi_{tie} = \max(\frac{\varphi_m}{6}, 6 \text{ mm}) \quad (31)$$

348 Spacing of tie bar (S_{tie}) can be calculated according to Eq. 32.

$$S_{tie} = \min(16\varphi_{tie}, 300 \text{ mm}) \quad (32)$$

349

350 2.3. Structural Design Optimization

351 2.3.1. Unified Particle Swarm Optimization (UPSO)

352 UPSO is a swarm based optimization proposed by Parsopoulos and Vrahitis [47] as a
353 upgraded version of Particle swarm optimization (PSO) [48, 49] based on the individual and
354 social behavior of flock of birds, school of fish etc. in their process of searching foods or
355 avoiding predators.

356 The algorithm begins with each particle assuming random position $S(t)$ and velocity $H(t)$.
 357 The position of each particle in the swarm represents a possible solution of the optimization
 358 problem. During the search process position of each particle gets updated with every iteration
 359 through a velocity update rule. Velocity update of each particle in every iteration depends on
 360 the three factor, such as, $a(t)$, i.e., the best position visited by the particle itself, $u(t)$, i.e., the
 361 best position ever visited by all the particles and $n(t)$, i.e., the best position visited by the
 362 neighbors of that particle. Thus, new position for each particle $S(t + 1)$ can be obtained by
 363 adding the updated velocity $H(t + 1)$ with previous position $S(t)$ (Eq. 33).

$$S(t + 1) = S(t) + H(t + 1), S(t + 1) \in [S_{min}, S_{max}] \quad (33)$$

364 The updated velocity can be obtained from Eq. 34.

$$H(t + 1) = \mu G(t + 1) + (1 - \mu)L(t + 1), H(t + 1) \in [-H_{max}, H_{max}] \quad (34)$$

$$G(t + 1) = \chi [H(t) + c_1 rand(0,1)(a(t) - S(t)) + c_2 rand(0,1)(u(t) - S(t))] \quad (35)$$

$$L(t + 1) = \chi [H(t) + c_1 rand(0,1)(a(t) - S(t)) + c_2 rand(0,1)(n(t) - S(t))] \quad (36)$$

365 μ is unification factor increasing from 0 to 1 exponentially according to Eq. 37

$$\mu(t) = \exp\left(\frac{t * \log 2}{MaxIt}\right) - 1 \quad (37)$$

366 Also, S_{max} and S_{min} are upper and lower limit for position respectively. V_{max} is upper limit for
 367 velocity = $(S_{max} - S_{min})/2$, $\chi = 0.729$, and $c_1 = c_2 = 2.05$ [50].

368 2.3.2. Beam and column design optimization

369 Beam and column design optimizations algorithm are developed by making suitable changes
 370 in the above mentioned UPSO algorithm. In the present study beams and columns has been
 371 optimized separately. The entire algorithm is divided into three steps accordingly.

372 (A) UPSO based beam design optimization

373 In the first steps all beams are optimized separately In case of beam design optimization

- 374 1. The input variables are considered as width (b), overall depth (D), diameter of main
375 bar at top (φ_t) and bottom (φ_b), no of compression bar support (n_{cs}) and mid span
376 (n_{cm}), no of tension bar at support (n_{ts}) and mid span (n_{tm}).
- 377 2. Only longitudinal reinforcement are optimized along with the cross sectional area.
378 Shear reinforcement are designed based on the optimized cross section and
379 longitudinal reinforcement amount.
- 380 3. The output variables are width, overall depth, diameter of bar at top and bottom of
381 section, number of bars at top and bottom for mid-span and support of section,
382 spacing of shear reinforcement at support and mid-span of section.
- 383 4. The following constraints are considered
- 384 a. $1.5b \leq D \leq 2b$
- 385 b. b and D are assumed in the multiple of 10 to take into account the practicality
386 aspects of construction.
- 387 c. Clear spacing of the bars should exceed the maximum aggregate size.
- 388 d. Moment and shear capacity of section should exceed the design moment and shear
389 of that section.
- 390 e. Total deflection (Eq. 14) should be less than $\frac{1}{250}$.

391 Detailed algorithm of UPSO based RC beam design optimization have been presented in
392 Algorithm 1 of Appendix II.

393 (B) UPSO based column design optimization

394 In the second step all column are optimized separately. In case of column design
395 optimization

- 396 1. The input design variables considered are as follows: width (b_c), depth (D_c), k_x , k_y ,
397 diameter of main bars (φ_m), number of main bars of columns in x and y directions
398 (n).

- 399 2. The output variables are considered as width (b_c), depth (D_c), kx , ky , diameter of
400 main bars (ϕ_m), number of main bars of columns in x and y directions (n), diameter
401 of tie bars and their spacing.
- 402 3. Constraints applied for columns are
- 403 a. b_c and D_c are assumed in the multiple of 10 to take into account the practicality
404 aspects of construction
- 405 b. Clear spacing of the bars should exceed the maximum aggregate size.
- 406 c. Limit for interaction ratio as given in equation Eq. 19 should be satisfied.

407 Detailed algorithm of UPSO based RC column design optimization have been presented in
408 Algorithm 2 of Appendix II.

409 (C) Combined beam-column design optimization

410 Eventually, all the individual optimization results of beams and columns are combined to
411 obtain optimized design for the entire building frame in the third step. Detail algorithm for
412 such action have been presented in Algorithm 3 of Appendix II. A flowchart for the entire
413 developed program is presented in Fig. 4.

414 2.3.3. Cost based objective function

415 Cost based objective function for beams and columns have been presented in Eq. 38.

$$F(\text{design_var}) = V_c C_c + V_s \rho_s C_s + A_f C_f \quad (38)$$

416 where $C_c = \text{Rs. } 5844/\text{m}^3$; $C_s = \text{Rs. } 68.508/\text{Kg}$; $C_f = 225/\text{m}^2$ (WB PWD schedule 2017
417 [51]).

418 Area of formwork (A_f) for beam and columns can be calculated from Fig. 5 as per Eq. 39 and
419 Eq. 40 respectively

$$(A_f)_{\text{beam}} = (b + 2D) * \text{length of beam} \quad (39)$$

$$(A_f)_{\text{column}} = (2b_c + 2D_c) * \text{length of column} \quad (40)$$

420

421 3.Numerical results and discussion

422 3.1. Problem definition

423 One G+8 L shaped building frame (Fig. 6a) and one G+10 U shaped building frame (Fig. 6b)
424 are considered to demonstrate the efficacy of proposed algorithm. The structures were
425 analyzed in STAADPro V8i [52] considering seismic loads, wind loads and gravity loads to
426 determine the most critical load case for each member. Now, an UPSO based algorithm has
427 been developed to obtain cost optimum design for beams and columns utilizing the design
428 loads obtained from STAAD Pro [52] for critical load cases without disrupting the safety
429 criteria. The designs of each beam and each column are optimized separately to consider the
430 contribution of all the design parameters responsible for beams and columns. The optimized
431 cost of all beams and columns are summed up to get the total optimized cost for each frame.
432 Efficient cost optimization algorithm of RC building frame depends on appropriate choice of
433 design parameters and internal parameters for optimization algorithm.

434 3.2. Design parameters

435 Important design parameter considered in the present study has been mentioned below:

- 436 i) Location of the structure : Kolkata, India (assumed)
- 437 ii) Thickness of outer wall and inner wall =250mm and 125 mm respectively (outer
438 walls and inner walls are assumed to be on outer and inner beam respectively).
- 439 iii) Unit weight of brick wall= 20 KN/m³
440 Unit weight of reinforced concrete= 25 KN/m³
- 441 iv) Floor finish load on roof= 1 KN/m²
- 442 v) Live on all roof= 1.5 KN/m²
443 Live load on all other floor= 3 KN/m²
- 444 vi) For wind load (IS 875(Part III) 2015) [44] (Appendix III)
445 $V_b = 50\text{m/s}$, $k_1 = 1$ (50 years life span) (Table IV, Appendix III), k_2 is function
446 of height (Table V of Appendix III) for terrain category 2, $k_3 = 1$ (for ground
447 slope $<3^\circ$), $k_4 = 1$ (ordinary RC frame).
448 $K_d = 1$, $K_a = 1$, $K_c = 0.9$.The velocity profile of wind load analysis used in the
449 analysis has been presented in Fig. 7.
- 450 vii) For seismic load (IS 1893(Part I)[45]

451 $Z = 0.16$ (Zone III), $I = 1$ (Ordinary building), $R = 3$ (ordinary moment resisting
452 frame), soil type: medium, $\frac{S_a}{g}$ can be calculated as per Fig. 2.

453 Seismic weight is calculated considering full dead load, no live load on roof and
454 half live load on all other floors

455 viii) Yield strength of reinforcement bar =415MPa and Characteristic strength of
456 concrete =25MPa (assumed)

457 ix) Beams and columns are designed considering load reversal due to seismic and
458 wind load cases. Reinforcement is placed only along the outer periphery of the
459 sections. Equal number of reinforcement is placed on all the four sides of the
460 columns. The space between two consecutive bars should be greater than
461 maximum aggregate size for convenience of the construction. Curtailment of extra
462 tensile bars in beam has been considered in present study (Fig. 8). Development
463 length of reinforcement of beam and columns at the end supports has not been
464 considered. In case of beam, different shear reinforcement spacing has been used
465 for support and mid span as required as all the beams are continuous with fixed
466 supports. Shear reinforcement for support has been designed for maximum shear
467 force of beam, while shear reinforcement at the mid span designed to carry
468 minimum shear.

469 x) Minimum and maximum diameter of main reinforcing bars for beams and
470 columns are 12mm and 32mm. The diameter of tie bar for shear in beams is 2
471 legged 8 mm and for columns are 8 mm.

472 3.3. Optimization parameters

473 1. Beams are optimized starting from bottom floor to top floor. The search space of the
474 beam design optimization has been restricted in such a way that the maximum value
475 of optimization design variables for a particular floor shall be equal to the optimized
476 design values obtained for the beams in the subsequent bottom floor (except for
477 ground floor). The minimum range of the design variables of all beams have been
478 kept same for all floors.

479 2. Columns are optimized starting from top floor to bottom floor. The search space of
480 the column design optimization has been restricted in such a way that the minimum
481 value of optimization design variables for a particular floor shall be equal to the
482 optimized design values obtained for the columns in the subsequent top floor (except

483 for topmost floor). The maximum range of the design variables of all beams have
484 been kept same for all floors.

485 3. Individual beam and column design optimization are performed separately for 10
486 numbers of experiments considering maximum iteration and swarm size 50 and 10
487 respectively. The experiment which exhibit minimum cost has been considered as the
488 optimized design for the respective beam and column.

489 4. In case of continuous beams, all spans have been designed considering the maximum
490 design moments and shear for the beam.

491 3.4. Numerical Results

492 3.4.1. L-shaped building frame

493 In this section developed UPSO based algorithm has been used to optimize the RC design of
494 the G+8 L-shaped building frame to have minimum cost. Search space of design variables
495 should be decided appropriately depending on the experience of the designer, as
496 inappropriate choice of search space can lead to large computational effort. Search space of
497 design variables considered in the study in case of beams are: $b \in [200,400]$, $D \in$
498 $[300,600]$, $\varphi_t \in [12,20]$, $\varphi_b \in [12,20]$, $n_{cs} \in [2,5]$, $n_{cm} \in [2,5]$, $n_{ts} \in [2,5]$, $n_{tm} \in [2,5]$.
499 Search space of design variables considered in the study in case of columns are: $b_c \in$
500 $[250,500]$, $D_c \in [250,500]$, $k_x \in [0.5,1.2]$, $k_y \in [0.5,1.2]$, $\varphi_m \in [12,25]$, $n \in$
501 $[2,4]$. Convergence curve for total cost for M20, M25, M30, and M35 grades of concrete
502 along with Fe 415 steel have been plotted in Fig. 9(a). Total cost of the building frame is
503 found to be varying within the range [3840101, 4014875] for Fe 415 steel and [3564230,
504 3942723] for Fe 500 steel for different grades of concrete. It can be observed that variation
505 among different grades of concrete is 4.5% and 10.7% for Fe 415 and Fe 500 steel. Next, Fig.
506 9(b) has been plotted showing the convergence curves of the total cost of concrete, total cost
507 formwork and total cost of steel through all the iterations for M20 grade of concrete and
508 Fe415 grade of steel. This will give designers a good insight regarding the inter-relationship
509 among these three parameters. Also, a bar diagram has been presented showing the
510 comparisons of total cost of the frame for different grades of steel (Fe415, Fe500) and
511 concrete (M20, M25, M30, M35) in Fig. 9(c). It can be seen that for all concrete grades, Fe
512 500 steel yields lower cost than Fe415 steel. Optimized design output for beams and columns
513 obtained from the algorithm has been reported respectively in Table 2 and Table 3 for
514 M20 concrete and Fe 415 steel. Beam design details of only three floors have been presented

515 for brevity (Table 2), whereas typical column design details for all the floors have been
516 presented (Table 3). In case of columns 6 mm diameter of links are considered throughout and
517 the spacing is 190mm c/c, 255mm c/c and 300mm c/c for 12 mm, 16 mm, and 20 mm
518 diameter main bars respectively.

519 Thus, the present algorithm has been found to be very flexible and effective to provide cost
520 optimized design for multistoried L shaped building, considering all the codal provisions (IS
521 456 [40]) and the practical considerations.

522 3.4.2. U-shaped building frame

523 In this section developed UPSO based algorithm has been used to optimize the RC design of
524 the G+10 U-shaped building frame to have minimum cost. Search space of design variables
525 should be decided appropriately depending on the experience of the designer, as
526 inappropriate choice of search space can lead to large computational effort. Search space of
527 design variables considered in the study in case of beams are: $b \in [200,250]$, $D \in$
528 $[500,300]$, $\varphi_t \in [12, 16]$, $\varphi_b \in [12, 16]$, $n_{cs} \in [2, 5]$, $n_{cm} \in [2, 5]$, $n_{ts} \in [2, 5]$, $n_{tm} \in [2, 5]$.
529 Search space of design variables considered in the study in case of columns are: $b_c \in$
530 $[250,400]$, $D_c \in [250,400]$, $k_x \in [0.5,1.2]$, $k_y \in [0.5,1.2]$, $\varphi_m \in [12,20]$, $n \in$
531 $[2,3]$. Convergence curve for total cost for M20, M25, M30, and M35 grades of concrete
532 along with Fe 415 steel have been plotted in Fig. 10(a). Total cost of the building frame is
533 found to be varying within the range [2813601, 2898791] for Fe 415 steel and [2805123,
534 2813406] for Fe 500 steel for different grades of concrete. Hence, the maximum variation in
535 total cost among different grades of concrete is found to be 3.03 % and 0.30 % for Fe 415 and
536 Fe 500 steel respectively. Fig. 10(b) represents the convergence curves of the total cost of
537 concrete, total cost formwork and total cost of steel through all the iterations for M25 grade
538 of concrete and Fe415 grade of steel. A bar diagram showing the total cost of frame was
539 outlined in Fig. 10(c) for various grades of concrete (M20, M25, M30, M35) and steel
540 (Fe415, Fe500). There is not much difference in the cost output for Fe 415 and Fe 500 as
541 observed in the previous problem. It can be seen that for all concrete grades, Fe 500 steel
542 yields lower cost than Fe415 steel. While beam design details of three different floors have
543 been presented in Table 4, column design details has been presented in Table 5 for typical
544 columns in all the floors. M25 concrete and Fe 415 steel are considered for design outputs of
545 both the tables. The diameter and spacing of links in columns are similar to the results
546 reported for L-shaped building frame. The present algorithm is adequately apt, suitably

547 adaptable and effectively potent to provide cost optimized design of reinforced concrete
548 buildings U- shaped building frame considering all the codal provisions(IS 456 [40])and
549 practical considerations.

550 3.5. Statistical Analysis

551 As optimization algorithms are based on random processes, possibility of coming up
552 with a different solution is quite common when a large number of experiments are involved.
553 However, the probability of the optimized objective function value to lie within an acceptable
554 range decides the robustness of the optimization algorithm. For that, a large number of
555 experiments are required and each and every solution should be checked whether it is in the
556 acceptable range of the optimum solution. It is a very time consuming and rigorous to
557 conduct a huge number of experiments (i.e. 5000 or 10,000) on the developed algorithm and
558 check every solution manually. In that case, the Monte Carlo simulation (Metropolis and
559 Ulam[53], Metropolis [54]) is used to assess the variations of the solutions of the developed
560 algorithm for large of number of experiments. However, the variations in results should be
561 within an acceptable range for an engineer to accept the results. Monte Carlo simulation is a
562 mathematical numerical method that uses random draws to perform calculations and complex
563 problems. The method was first introduced by Stanislaw Ulam (Eckhardt [55]) and is based
564 on the game of dice, roulette etc. Monte Carlo simulation can be used create large number of
565 solutions of the problem in hand numerically from a small available number of solutions
566 based on a normal distribution curve or bell curve. Then the normal distribution curve can be
567 used to obtain the forecast of the favorable solution and its probability. The probability of the
568 occurrence of the favourable solution among a large number of experiments can be estimated
569 in the normal distribution curve. This decides the robustness of the developed algorithm.

570 In the present study aMonte Carlo simulation for 5000 probable solutions (total cost of
571 frames) of the developed algorithm was performed using MS excel.The expression for
572 probable solution of each simulation was worked out using the following expression in Eq.
573 41.

$$tot_cost_{i+1} = tot_cost_i \times e^{D_r+R}, i = 1,2, \dots, 5000 \quad (41)$$

574 where, D_r and R can be calculated from Eq. 42 and Eq. 43 respectively.

$$D_r = \mu_E - \sigma^2/2 \quad (42)$$

$$R = \sigma \times \text{normsinv}(\text{rand}(0,1)) \quad (43)$$

575 Where, *normsinv* is an excel function which returns probability corresponding to the
 576 standard normal distribution with a mean of zero and a standard deviation of one. μ_E and σ
 577 are respectively mean and standard deviation of the 10 number of available total cost values.
 578 μ_E is considered as *tot_cost_i* for calculating the values for first simulation.

579 Summary of results of 10 numbers of experiments obtained employing the optimization
 580 algorithm along with the key solution of Monte Carlo simulation is presented in Table 6 and
 581 Table 7 for L-shaped building frame and U-shaped building frame respectively. Total cost of
 582 L-shaped and U-shaped building frame are found to be lying in the ranges of [3792373.03,
 583 3923637.97] and [2833889.28, 2887321.15] respectively after 5000 simulations. These
 584 ranges are divided into 20 equal divisions. The probability of total cost falling within each
 585 interval was estimated considering 5000 forecasted solutions. These probability values
 586 obtained for 20 intervals are plotted in Fig. 11 and Fig. 12 for L-shaped and U-shaped frames
 587 respectively. Both the plots clearly depict the nature of a normal distribution curve. The most
 588 likely solution is at the middle of the curves, meaning there is an equal chance that the actual
 589 solution will be higher or lower than that value. The key percentile shows the likely values of
 590 the total cost of frames. For example, the key percentile value against the 25% shows that
 591 there is 25% chance that the developed algorithm will provide this total cost. Similarly, key
 592 percentiles for 50% and 75% chance have also been evaluated. Key percentile values are
 593 presented in Table 6 and Table 7 for L-shaped and U-shaped building frame
 594 respectively. Also, the total cost corresponding to 99% for both the frames also proves that
 595 there is negligible scope for design failure by the developed algorithm. Loss percentile is
 596 calculated keeping the maximum total cost to be Rs. 39, 00,000 and Rs. 28, 80,000 for L-
 597 shaped and U-shaped frame respectively. The loss percentile shows that there is only 2%
 598 chance of the total cost to exceed Rs. 39, 00,000 (Table. 6) for L-shaped frame and 0.6%
 599 chance to exceed Rs. 28, 80,000 (Table 7) for U-shaped frame, which are very close to first
 600 simulation values. The loss percentages are found to be very negligible. Therefore, the
 601 optimum design of the frames using the developed algorithm is not only found safe in every
 602 experiments but it also provide an optimum overall cost almost every time.

603 3.6. Feasibility analysis in terms of safety

604 In the present algorithm beams and columns are optimized separately and added later to
605 obtain the optimized design for the entire frame. Therefore, the stiffness redistribution among
606 beams and columns due to varying sizes of them in each iteration of the optimization have
607 not been taken into account. Thus, from mathematical point of view slight error has been
608 imparted into the analysis. In the present algorithm a few measures have been taken to ensure
609 the safety of the structures. The analysis and preliminary design of the buildings are
610 performed in STAAD Pro, in such way that sizes of all beams and columns has been chosen
611 in a conservative manner. It was then made sure that design was safe as per design standard.
612 Next, design forces (shear force, moment and axial forces) have been taken from the
613 conservative STAAD Pro model and fed into the developed optimization algorithm in
614 MATLAB. In that way the sizes of beams and columns only reduced during optimization
615 procedure as can be seen from Table 2-5. The design force is kept same as the preliminary
616 analysis of STAAD Pro. In that way, it has been made sure that design was always carried
617 out for design forces higher than the actual design forces obtained during the course of the
618 optimization program. After optimization is done, optimized member sizes are incorporated
619 in STAADPro model to compare the design forces of optimized structures with actual
620 STAADPro model. Table 8-9 have been presented showing the comparison between the
621 design forces of the structures before and after optimization for a typical fourth floor of one
622 building (L-shaped). Actual design forces and moments of optimized structure are observed
623 to be significantly lower than the design forces and moments of the structure before
624 optimization. So, the optimized design has been indeed carried out for higher design forces
625 and moments than the actual. Therefore, the aforementioned error has not influence the safety
626 of the buildings significantly enough to violate the safety criteria provided by the design
627 standard. So, from practical civil engineering point of view the design results obtained from
628 present algorithm is feasible and safe enough to be used for cost-optimum design of RC
629 building frame.

630 **4.Conclusion**

631 In the present study, an UPSO based optimization algorithm has been developed in
632 MATLAB [56]environment to find cost optimum design of reinforcement concrete building
633 frame considering the codal specifications of safety and serviceability of IS 456 [33] along
634 with the consideration for the construction requirements in practical field.

635 Two building frames namely G+8 L-shaped frame and G+10 U-shaped frame have been
636 adopted to demonstrate the efficacy of the developed algorithm. Popular design and analysis
637 software STAADPro. V8i [52] has been used to obtain the design forces (bending moments,
638 shear forces and axial forces) in critical sections of all the beams and columns considering the
639 effects of gravity loads, wind loads and seismic loads as per the specifications of the
640 respective Indian Standards. Next, each beam and column are optimized separately
641 employing UPSO based algorithm. Thus, total optimized cost of the frames has been obtained
642 by adding up all the optimized costs of these beams and columns. Numerical results have
643 revealed that the present algorithm is capable of providing cost optimized design of RC
644 frames of any shape and height with profound accuracy. Further, Monte Carlo
645 simulation performed assures the consistency and robustness of the developed algorithm with
646 almost hundred percent design success. This further confirms that the algorithm can be
647 effectively used for optimal design of any type of reinforced concrete buildings having
648 different design constraints. Only the design variables and constraints need to be modified to
649 adapt to the particular building problem. Overall, the present UPSO based algorithm has been
650 found to be very effective in finding cost optimum design of RC frame having any planner
651 irregularity and any number of floors. The positive findings of the research will encourage the
652 future researchers to improve the present algorithm to incorporate more minute reinforcement
653 details such as development length, ductile detailing etc. Also, finite element method can be
654 incorporated within the algorithm to obtain the design forces directly instead of relying on
655 commercial design software. In that way accuracy of the results can be improved further.

656

657 **Data availability statement**

658 All the required data presented in the manuscript itself. Any further data important to the
659 readers can be made available as per their request.

660 **Acknowledgement**

661 The author wish to acknowledge anonymous reviewers for their valuable suggestions and
662 comments. The authors are grateful to department of Civil Engineering, IIT Kharagpur to
663 provide the necessary infrastructure to carry out the research work.

664 **Conflict of interest**

665 On behalf of all authors, the corresponding author states that there is no conflict of interest.

666 **Replication of results**

667 The authors hereby state that they are willing to share all the codes and numerical data needed
668 to reproduce the figures.

669

670 **References**

- 671 [1] Milajić, A., Pejicic, G., and Beljakovic, D. (2013). “Optimal Structural Design of
672 Reinforced Concrete Structures – Review of Existing Solutions.” *Archives for*
673 *Technical Sciences*, 9(1), 53–60.
- 674 [2] Hasencebi, O., Teke, T., and Pekcan, O. (2013). “A bat-inspired algorithm for
675 structural optimization.” *Computers and Structures*, 128, 77-90.
- 676 [3] Wang, L., Zhang, H. and Zhu, M. (2020). “A new Evolutionary
677 StructuralOptimization method and application for aided design to reinforced
678 concretecomponents.” *Struct Multidisc Optim.* [https://doi.org/10.1007/s00158-020-](https://doi.org/10.1007/s00158-020-02626-z)
679 [02626-z](https://doi.org/10.1007/s00158-020-02626-z).
- 680 [4] Lu, H., Gilbert, M. and Tyas, A. (2019). “Layout optimization of building frames
681 subject to gravity and lateral load cases”. *Struct Multidisc Optim* 60, 1561–1570.
- 682 [5] Lee, J. (2019). “Multi-objective optimization case study with active and passive
683 design in building engineering.” *Struct Multidisc Optim* 59, 507–519.
- 684 [6] Zegard, T., Hartz, C., Mazurek, A. (2020). “Advancing building engineering through
685 structural and topology optimization.” *Struct Multidisc Optim.*
686 <https://doi.org/10.1007/s00158-020-02506-6>.
- 687 [7] Prakash, A., Agarwala, S. K., and Singh, K. K. (1988). “Optimum design of
688 reinforced concrete sections.” *Computers and Structures*, 30(4), 1009–1011.
- 689 [8] Chakrabarty, B. K. (1992). “Models for optimal design of reinforced concrete
690 beams.” *Computers and Structures*, 42(3), 447–451.
- 691 [9] Coello, C. C., Hernández, F. S., and Farrera, F. A. (1997). “Optimal design of
692 reinforced concrete beams using genetic algorithms.” *Expert Systems with*
693 *Applications*, 12(1), 101–108.
- 694 [10] Rajeev, S., and Krishnamoorthy, C. S. (1998). “Genetic algorithm-based
695 methodology for design optimization of reinforced concrete frames.” *Computer-*
696 *Aided Civil and Infrastructure Engineering*, 13(1), 63–74.

- 697 [11] Dole, M. R., Ronghe, G. N., and Gupta, L. M. (2000). "Optimum design of
698 reinforced concrete beams using polynomial optimization technique." *Advances in*
699 *Structural Engineering*, 3(1), 67–79.
- 700 [12] De Medeiros, G. F., and Kripka, M. (2013). "Structural optimization and
701 proposition of pre-sizing parameters for beams in reinforced concrete buildings."
702 *Computers and Concrete*, 11(3), 253–270.
- 703 [13] Niğdeli, S. M., and Bekdaş, G. (2017). "Optimum design of RC continuous beams
704 considering unfavourable live-load distributions." *KSCE Journal of Civil*
705 *Engineering*, 21(4), 1410–1416.
- 706 [14] Uz, M. E., Sharafi, P., Askarian, M., Fu, W., and Zhang, C. (2018). "Automated
707 layout design of multi-span reinforced concrete beams using charged system search
708 algorithm." *Engineering Computations*, 35(3), 1402–1413.
- 709 [15] Ferreira, C. C., Barros, M. H. F. M., and Barros, A. F. M. (2003). "Optimal design
710 of reinforced concrete T-sections in bending." *Engineering Structures*, 25(7), 951–
711 964.
- 712 [16] Preethi, G., and Arulraj, P. G. (2016). "Optimal Design of Axially Loaded RC
713 Columns." *Bonfring International Journal of Industrial Engineering and*
714 *Management Science*, 6(3), 78–81.
- 715 [17] Bekdaş, G., and Niğdeli, S. M. (2016). "Optimum design of reinforced concrete
716 columns employing teaching-learning based optimization." *Challenge Journal of*
717 *Structural Mechanics*, 2(4), 216–219.
- 718 [18] Aldwaik, M. and Adeli, H. (2016). "Cost optimization of reinforced concrete flat
719 slabsof arbitrary configuration in irregular highrise building structures." *Struct*
720 *MultidiscOptim*54, 151–164.
- 721 [19] Aldwaik, M. and Adeli, H. (2014). "Advances in optimization of
722 highrisebuildingstructures." *Struct Multidisc Optim*50, 899–919.
- 723 [20] Chaudhuri, P. and Maity, D. (2020). "Cost optimization of rectangular RC footing
724 using GA and UPSO." *Soft Computing*, 24 (January), 709–721

- 725 [21] Kaveh, A., and Behnam, A. F. (2013). “Design optimization of reinforced concrete
726 3D structures considering frequency constraints via a charged system search.”
727 *ScientiaIranica*, Elsevier B.V., 20(3), 387–396.
- 728 [22] Bekdaş, G., and Nigdel, S. M. (2014). “Optimization of RC frame structures
729 subjected to static loading.” *11th World Congress on Computational Mechanics*,
730 *WCCM 2014, 5th European Conference on Computational Mechanics, ECCM*
731 *2014 and 6th European Conference on Computational Fluid Dynamics, ECFD*
732 *2014*, (Wccm Xi), 3869–3875.
- 733 [23] Aga, A. A. A., and Adam, F. M. (2015). “Design Optimization of Reinforced
734 Concrete Frames.” *Open Journal of Civil Engineering*, 05(01), 74–83.
- 735 [24] Gharehbaghi, S., and Khatibinia, M. (2015). “Optimal seismic design of reinforced
736 concrete structures under time- history earthquake loads using an intelligent hybrid
737 algorithm.” *Earthquake Engineering and Engineering Vibration*, 14(1), 97–109.
- 738 [25] Esfandiary, M. J., Sheikholarefin, S., and Bondarabadi, H. A. R. (2016). “A
739 combination of particle swarm optimization and multi-criterion decision-making
740 for optimum design of reinforced concrete frames.” *International Journal of*
741 *Optimization in Civil Engineering*, 6(2), 245–268.
- 742 [26] Kulkarni, A., and Bhusare, V. (2017). “Structural optimization of reinforced
743 concrete structures Structural Optimization of Reinforced Concrete Structures.”
744 *International Journal of Engineering Research & Technology (IJERT)*, 5(March),
745 123–127.
- 746 [27] Bekas, G. K., and Stavroulakis, G. E. (2017). “Machine Learning and Optimality in
747 Multi Storey Reinforced Concrete Frames.” *Infrastructures*, 2(2), 6.
- 748 [28] Tapao, A., and Cheerarot, R. (2017). “Optimal parameters and performance of
749 artificial bee colony algorithm for minimum cost design of reinforced concrete
750 frames.” *Engineering Structures*, Elsevier Ltd, 151, 802–820.
- 751 [29] Esfandiari, M. J., Urgessa, G. S., Sheikholarefin, S., and Manshadi, S. H. D. (2018).
752 “Optimum design of 3D reinforced concrete frames using DMPSO algorithm.”
753 *Advances in Engineering Software*, 115(September 2017), 149–160.

- 754 [30] RazmaraShooli, A., Vosoughi, A.R. and Banan, M.R. (2019). “A mixed GA-PSO-
755 based approach for performance-based design optimization of 2D reinforced
756 concrete special moment-resisting frames.” *Applied Soft Computing Journal*,
757 85(105843).
- 758 [31] Milajić, A., Beljakovic, D., and Culic, N. (2014). “Optimal Structural Design Based
759 on Applicability in Practice.” *In conference proceedings of People, People,*
760 *Buildings and Environment*, Kroměříž, Czech Republic, 306–315.
- 761 [32] Milajić, A., Prokic, A., Beljakovic, D., and Pejicic, G. (2015). “Quantitative method
762 for evaluating applicability of designed reinforcement pattern.”
763 *Kvantitativnimetodzaocjenuprimjenljivostiprojektiraneshemearmiranja*, 22(1),
764 119–124.
- 765 [33] Nanda, B., Maity, D., Maiti, D.K. (2014). “Modal parameter based inverse
766 approach for structural joint damage assessment using unified particle swarm
767 optimization.” *Applied Mathematics and Computation*, 242(1), 407-422.
- 768 [34] Nanda, B., Maity, D., Maiti, D.K. (2014). “Damage assessment from curvature
769 mode shape using unified particle swarm optimization.” *Structural Engineering*
770 *and Mechanics Volume*, 52(2), 307-322.
- 771 [35] Mohan, S. C., Maiti, D. K and Maity, D. (2013) “Structural damage assessment
772 using FRF employing particle swarm optimization” *Applied Mathematics and*
773 *Computation*, 219 (20), 10387-10400.
- 774 [36] Barman S.K., Maiti D.K., Maity D. (2020) Damage Detection of Truss Employing
775 Swarm-Based Optimization Techniques: A Comparison. In: Venkata Rao R., Taler
776 J. (eds) *Advanced Engineering Optimization Through Intelligent Techniques.*
777 *Advances in Intelligent Systems and Computing*, 949.21-37 Springer, Singapore.
- 778 [37] Barman, S. K., Jebieshia, T. R., Tiwari, P, Maiti, D.K. and Maity, D. (2019) “Two-
779 Stage Inverse Method to Detect Delamination in Composite Beam Using Vibration
780 Responses” *AIAA Journal*. 57 (3). 1312-1322.
- 781 [38] Mishra, M., Barman, S. K, Maity, D and Maiti, D. K. (2020). “Performance
782 Studies of 10 Metaheuristic Techniques in Determination of Damages for Large-

- 783 Scale Spatial Trusses from Changes in Vibration Responses.” *Journal of*
784 *Computing in Civil Engineering*, 34 (2), 04019052.
- 785 [39] Parsopoulos, K.E., Kariotou, F., Dassios, G. and Vrahatis, M.N. (2009). ‘Tackling
786 magnetoencephalography with particle swarm optimization’. *International Journal*
787 *of Bio-Inspired Computation*, 1(1–2), 32-49
- 788 [40] IS 456 (2000). *Plain and Reinforced Concrete - Code of Practice*, Bureau of Indian
789 Standards, New Delhi, India
- 790 [41] IS 875 (Part I) (1987). *Code of practice for design loads (other than earthquake)for*
791 *buildings and structures: part 1 dead loads - unit weights of building material and*
792 *stored materials*, Bureau of Indian Standards, New Delhi, India
- 793 [42] IS 875 (Part II) (1987). *Code of practice for design loads (other than earthquake)*
794 *for buildings and structures: part 2 imposed loads*, Bureau of Indian Standards,
795 New Delhi, India
- 796 [43] SP 64 (Part III) (2001). *Explanatory handbook on Indian standard code of practice*
797 *for design loads (other than earthquake) for buildings and structures*, Bureau of
798 Indian Standards, New Delhi, India
- 799 [44] IS 875 (Part III) (2015). *Design loads (other than earthquake) for buildings and*
800 *structures - code of practice - part 3 wind loads*, Bureau of Indian Standards, New
801 Delhi, India
- 802 [45] IS 1893 (Part I) (2016). *Criteria for earthquake resistant design of structures - part*
803 *1: general provisions and buildings*, Bureau of Indian Standards, New Delhi, India
- 804 [46] IS 875 (Part V) (2015). *Code of practice for design loads (other than*
805 *earthquake)for buildings and structures: part 5special loads and load*
806 *combinations*, Bureau of Indian Standards, New Delhi, India
- 807 [47] Parsopoulos, K. E., and Vrahatis, M. N. (2005). “Unified Particle Swarm
808 Optimization for Solving Constrained Engineering Optimization Problems.”
809 *Advances in natural computation*, Springer, Springer Berlin Heidelberg, Berlin,
810 Heidelberg, 582–591.

- 811 [48] Kennedy, J. and Eberhart, R. (1995). "Particle swarm optimization." *International*
812 *Conference on Neural Networks, IEEE, Australia.*
- 813 [49] Perez, R. E., and Behdinan, K. (2007). "Particle swarm approach for structural
814 design optimization." *Computers and Structures*, 85(19), 1579-1588.
- 815 [50] Parsopoulos, K. E., and Vrahatis, M. N. (2010). *Particle Swarm Optimization and*
816 *Intelligence*, Vol. 270, 2010. doi:10.4018/978-1-61520-666-7.
- 817 [51] WB PWD schedule.(2017) *Schedule of rates, volume I: building works*. Public
818 Works Department (PWD), Government of West Bengal (WB), India
- 819 [52] STAAD Pro V8i (2017). *Select series 6*, Bentley Systems, Inc. PA, USA.
- 820 [53] Metropolis, N., and Ulam, S. (1949). "The Monte Carlo Method." *Journal of the*
821 *American Statistical Association*, 44(247), 335-341. doi:10.2307/2280232
- 822 [54] Metropolis, N. (1987). The beginning of the Monte Carlo method. *Los Alamos*
823 *Science* 15: 125-130
- 824 [55] Eckhardt, R. (1987). "Stan Ulam, John Von Neumann, and the Monte Carlo
825 method." *Los Alamos Science*, 15, 131--136.
- 826 [56] MATLAB (2015), The Mathworks Inc. USA.
- 827

828 **APPENDIX I. Notation**

829 *The following symbols have been used in this paper:*

830 A_h = Horizontal acceleration coefficient

831 W = Seismic weight of building

832 Z = Seismic zone factor

833 $\frac{S_a}{g}$ = Design acceleration coefficient

834 T_a = Natural period of building

835 H_{bl} = Height of the building from plinth level

836 D_{bl} = Base dimension of the building in the direction of earthquake
837 shaking

838 R = Response reduction factor

839 I = Importance factor

840 p_d = Design wind pressure

841 K_d = Wind directionality factor

842 K_a = Area averaging factor

843 K_c = Combination factor

844 V_z = Design wind speed

845 V_b = Basic wind speed

846 k_1 = Probability factor

847 k_2 = Terrain roughness and height factor

848 k_3 = Topology factor

849 $k_4 =$ Importance factor for cyclonic region

850 $b =$ Width of the beam

851 $D =$ Overall depth of the beam

852 $d_e =$ Effective depth of the beam

853 $d' =$ depth of compression reinforcement from compression face of
854 beam.

855 $l_c =$ effective length of column

856 $D_c =$ width/ depth of the column

857 $\frac{x_{umax}}{d_e} =$ Limiting neutral axis depth factor for beam.

858 $f_{ck} =$ Grade of concrete

859 $f_y =$ Grade of steel reinforcement

860 $A_{st} =$ Area of tensile reinforcement for beam

861 $A_{sc} =$ Area of compressive reinforcement for beam

862 $\tau_v =$ Nominal shear strength

863 $\tau_c =$ Shear strength of concrete

864 $\tau_{cmax} =$ Maximum shear strength of concrete

865 $s_v =$ Spacing of shear reinforcement for beam

866 $A_{sv} =$ Total cross sectional area of the stirrup legs

867 $a_s =$ Short term deflection of beam

868 $a_{cs} =$ Deflection of beam due to shrinkage

869 $a_{cc} =$ Deflection of beam due to creep

870 E_c = Short term elasticity modulus for beam

871 I_{eff} = Effective moment of inertia for short term deflection of beam

872 I_r = Moment of inertia of cracked section of beam

873 I_{gr} = Gross moment of inertia of beam

874 M_r = Cracking moment

875 f_{cr} = Modulus of rupture of concrete

876 y_t = Distance from the centroidal axis of gross section, neglecting the
877 reinforcement, to extreme fibre in tension

878 M = Maximum moment under service load for beam

879 z = Lever arm of the beam section

880 x = Depth of the neutral axis for beam

881 b_w = Breadth of web for beam

882 b_b = Breadth of compression face for beam

883 f_3 = Constant depending upon the support condition of beam

884 φ_{cs} = Shrinkage curvature for beam

885 f_4 = Factor depending on percentage of tensile and compressive
886 reinforcement for beam

887 ϵ_{cs} = Ultimate shrinkage strain of concrete for beam

888 l = Length of the span of beam

889 $a_{i,cc}$ = Initial plus creep deflection of beam due to permanent loads

890 E_{ce} = Young's modulus of concrete to calculate $a_{i,cc}$

891 E_c = Actual Young's modulus of concrete to calculate short term
892 deflection

893 θ = Creep coefficient

894 D_c =Depth of the column

895 b_c =width of column

896 l_c =Length of the column.

897 A_c = Area of the concrete in column section

898 A_{scc} = Area of reinforcement in column

899 φ_m = Diameter of the main bar of the column

900 iter = number of iterations in each experiment for the developed
901 MATLAB program.

902 max_iter = maximum number of iterations in each experiment for the
903 developed MATLAB program.

904 exp = number of experiments, i.e., 1,2,3,....

905 $nexp$ = maximum number of experiments considered.

906 V_c = Volume of gross concrete work of beam / column in cubic meters.

907 V_s =Volumeof steel reinforcement of beam / column in cubic meters.

908 ρ_s = Density of steel i.e. 7850 Kg/m³.

909 C_c = Cost of reinforced concrete work per cubic meters.

910 C_s = Cost of steel reinforcement per Kg.

911 C_f = Cost of formwork per square meters.

912

913 **APPENDIX II.** Algorithm of the developed program

914
915
916
917
918
919
920
921
922
923
924
925
926
927
928
929
930
931
932
933
934
935
936
937
938
939
940
941
942
943
944
945
946
947
948
949
950
951
952
953
954
955
956
957
958

Algorithm1 Beam design optimization

Input: $SS=10, dim=8 (b, D, \varphi_t, \varphi_b, n_{cs}, n_{cm}, n_{ts}, n_{tm}), GM=1, MaxIt=50, nexp=10, Smin = [b_{min}, D_{min}, \varphi_{min}, \varphi_{min}, n_{min}, n_{min}, n_{min}, n_{min}], Smax = [b_{max}, D_{max}, \varphi_{max}, \varphi_{max}, n_{max}, n_{max}, n_{max}, n_{max}]$

Output: Optimized variable $S_{opt,beam}$, Optimized cost $F_{opt,beam}$

```

1:  for  $Ex=1:nexp$ 
2:  Initialization:  $t \leftarrow 0$ 
3:  Initialization: Swarm position  $S(t): b \in [b_{min}, b_{max}], D \in [D_{min}, D_{max}]$ 
    $\varphi_t, \varphi_b \in \varphi, \varphi = [12, 16, 20, 25, 32], \varphi_t, \varphi_b \in [\varphi_{min}, \varphi_{max}], n_{cs}, n_{cm}, n_{ts}, n_{tm} \in [n_{min}, n_{max}]$ 
   Swarm velocity:  $H(t) \in [-H_{max}, H_{max}]$ 
4:  Maintain: Constraint for beam design of Section 2.3.2
5:  Perform: Beam design (flexure and shear), deflection check (Section 2.2.1)
6:  Calculate: Cost of beam  $F_{beam}$  (Eq. 38)
7:  Calculate: best positions  $p(t), g(t)$  and  $l(t)$ 
8:  Calculate: best particle  $x_{opt,beam}$ , corresponding objective function  $f_{xopt,beam}$ 
9:  Initialization:  $STOP=0$ 
10: while  $STOP=0$  do
11:  Update:  $t \leftarrow t+1$ 
12:  Calculate:  $\mu(t)$  (Eq.37)
13:  Update:  $H(t)$  (Eq.34) and  $S(t)$  (Eq.33)
14:  Maintain: Constraint for beam design of Section 2.3.2
15:  Perform: Beam design (flexure and shear), deflection check (Section 2.2.1)
16:  Calculate: Cost of beam  $F_{beam}$  (Eq.38)
17:  Update:  $p(t), g(t)$  and  $l(t)$ 
18:  Update:  $x_{opt,beam}, f_{xopt,beam}$ 
19:  if  $f_{xopt} \leq GM$  or  $t=MaxIt$  then
20:     $STOP=1$ 
21:  else
22:    Goto step 11
23:  end if
24: end while
25: Calculate: Optimize variable  $S_{opt}$ , Optimized cost  $F_{xopt}$ 
26: end for
27: Calculate: Final Optimize variable  $S_{opt,beam}$ , Optimized cost  $F_{xopt,beam}$  (best out of  $nexp$ 
experiments)

```

959
960
961
962
963
964
965
966
967
968
969
970
971
972
973
974
975
976
977
978
979
980
981
982
983
984
985
986
987
988
989
990
991
992
993
994
995
996
997
998
999

Algorithm2 Column design optimization

Input: $SS=10, dim=6 (b_c, D_c, k_x, k_y, \varphi_m, n), GM=1, MaxIt=50, nexp=10, Smin = [b_{c,min}, D_{c,min}, k_{x,min}, k_{y,min}, \varphi_{min}, n_{min}], Smax = [b_{c,max}, D_{c,max}, k_{x,max}, k_{y,max}, \varphi_{max}, n_{max}]$

Output: Optimized variable $S_{opt,column}$, Optimized cost $F_{opt,column}$

- 1: **for** $Ex=1:nexp$
- 2: Initialization: $t \leftarrow 0$
- 3: Initialization: Swarm position $S(t)$:
 $b_c \in [b_{c,min}, b_{c,max}], D_c \in [D_{c,min}, D_{c,max}], k_x \in [k_{x,min}, k_{x,max}], k_y \in [k_{y,min}, k_{y,max}]$
 $\varphi_m \in \varphi, \varphi = [12,16,20,25,32], \varphi_m \in [\varphi_{min}, \varphi_{max}], n \in [n_{min}, n_{max}]$
- Swarm velocity $H(t) \in [-H_{max}, H_{max}]$
- 4: Maintain: Constraint for column design of Section 2.3.2
- 5: Perform: Column design for longitudinal reinforcement and lateral ties (Section 2.2.2)
- 6: Calculate: Cost of column F_{column} (Eq.38)
- 7: Calculate: best positions $p(t), g(t)$ and $l(t)$
- 8: Calculate: best particle $x_{opt,column}$, corresponding objective function $f_{xopt,column}$
- 9: Initialization: $STOP=0$
- 10: **while** $STOP=0$ **do**
- 11: Update: $t \leftarrow t+1$
- 12: Calculate: $\mu(t)$ (Eq.37)
- 13: Update: $H(t)$ (Eq.34) and $S(t)$ (Eq.33)
- 14: Maintain: Constraint for column design of Section 2.3.2
- 15: Perform: Column design for longitudinal reinforcement and lateral ties (Section 2.2.2)
- 16: Calculate: Cost of column F_{column} (Eq.38)
- 17: Update: $p(t), g(t)$ and $l(t)$
- 18: Update: $x_{opt,column}, f_{xopt,column}$
- 19: **if** $f_{xopt} \leq GM$ or $t=MaxIt$ **then**
- 20: $STOP=1$
- 21: **else**
- 22: Gotostep11
- 23: **end if**
- 24: **end while**
- 25: Calculate: Optimize variable S_{opt} , Optimized cost F_{xopt}
- 26: **end for**
- 27: Calculate: Final Optimize variable $S_{opt,column}$, Optimized cost $F_{xopt,column}$ (best out of $nexp$ experiments)

1000
1001
1002

1003

1004

1005

1006
1007
~~1008~~
1009
1010
1011
1012
1013
1014
1015
1016
1017
1018
1019
1020
1021
~~1022~~
~~1023~~
1024

Algorithm3 Combined optimized cost of frame

Input: X_{min}, X_{max} (as per Section.3.4), Design forces: Moment and shear force for beams, Axial forces and biaxial moments for columns from STAAD

Output: Optimized designs: $X_{opt,beam}$, $X_{opt,column}$, Optimized cost: $F_{opt,beam}$, $F_{opt,column}$

- 1: Beam design optimization (**Algorithm 1**): One by one from ground floor to top floor. Update X_{min}, X_{max} for each floor (Section 3.3).
 - 2: Column design optimization (**Algorithm 2**): One by one from top floor to ground floor. Update X_{min}, X_{max} for each floor (Section 3.3).
 - 3: Find out optimum beam design and column design
 - 3: Calculate total optimize cost of frame = $\sum F_{opt,beam} + \sum F_{opt,column}$
-

1025 **APPENDIX III**

1026

1027 **Parameters used in design of beam:**

1028 *For doubly reinforced beam*

1029 Table I Stress in compression reinforcement (f_{sc}), (N/mm²) in doubly reinforced beams with cold
1030 worked bars

SP16 Table F		
d'/d	$f_y = 415 \text{ N/mm}^2$	$f_y = 500 \text{ N/mm}^2$
0.05	355	424
0.1	353	412
0.15	342	395
0.2	329	370

1031

1032 *For design of beam in shear*

1033 Design shear strength $\tau_c = \frac{0.85\sqrt{0.8f_{ck}(\sqrt{1+5\beta}-1)}}{6\beta}$, $\beta = \frac{0.8f_{ck}}{6.89P_t} \geq 1$, $P_t = \frac{100A_{st}}{bd}$, A_{st} is area of tensile reinforcement,

1034 b, d are width and effective depth. f_{ck} = Grade of concrete

1035

1036 Table II Maximum Shear Stress ($\tau_{c,max}$), N/mm² (IS 456)

Table 24 (Clauses B-2.3, B-5.2.3, B-5.2.3, t, B.5.5,1 and B-6.3.1)						
f_{ck} (N/mm ²)	15	20	25	30	35	40
$\tau_{c,max}$ (N/mm ²)	2.5	2.8	3.1	3.5	3.7	4

1037

1038 *For deflection check in beam*

1039 $f_3 = 0.5$ for cantilevers, 0.125 for simply supported members, 0.086 for continuous at one end and 0.063 for fully
1040 continuous members

1041 $f_4 = 0.72 \frac{P_t - P_c}{\sqrt{P_t}} \leq 1.0$ for $0.25 \leq P_t - P_c \leq 1.0$

1042 $= 0.65 \frac{P_t - P_c}{\sqrt{P_t}} \leq 1.0$ for $P_t - P_c \geq 1.0$, $P_t = \frac{100A_{st}}{bd}$, $P_c = \frac{100A_{sc}}{bd}$, A_{sc} is area of compressive reinforcement.

1043

1044 **Parameters used in design of column:**

1045

1046 Table III Salient points on the design stress-strain curve for cold-worked bars

SP 16 (Table A)			
$f_y = 415 \text{ N/mm}^2$		$f_y = 500 \text{ N/mm}^2$	
Strain	Stress (N/mm ²)	Strain	Stress (N/mm ²)
0.00144	288.7	0.00174	347.8
0.00163	306.7	0.00195	369.6
0.00192	324.8	0.00226	391.3
0.00241	342.8	0.00277	413
0.00276	351.8	0.00312	423.9
0.0038	360.9	0.00417	434.8

1047

1048
 1049
 1050
 1051
 1052

Parameters used in wind analysis:

Table IV Risk coefficient (k_1) for structures in different wind speed zones

IS 875 part 3 2015 Table 1 (Clause 6.3.1)							
Class of structures	Design life of structures (years)	k_1 factor for basic wind speed (m/s)					
		33	39	44	47	50	55
All general structures	50	1.00	1.00	1.00	1.00	1.00	1.00
Temporary structures	5	0.82	0.76	0.73	0.71	0.70	0.67
Structures with low degree of hazards	25	0.94	0.92	0.91	0.90	0.90	0.89
Important building	100	1.05	1.06	1.07	1.07	1.08	1.08

1053
 1054
 1055

Table V Factors to obtain design wind speed variation with height in different terrains (k_2)

IS 875 part 3 2015 Table 2 (Clause 6.3.2.2.)				
Height (m)	Height multiplier (k_2) for terrain category			
	1	2	3	4
10	1.05	1.00	0.91	0.80
15	1.09	1.05	0.97	0.80
20	1.12	1.07	1.01	0.80
30	1.15	1.12	1.06	0.97
50	1.2	1.17	1.12	1.1
100	1.26	1.24	1.2	1.2
150	1.3	1.28	1.24	1.24
200	1.32	1.3	1.27	1.27
250	1.34	1.32	1.29	1.28
300	1.35	1.34	1.31	1.3
350	1.35	1.35	1.32	1.31
400	1.35	1.35	1.34	1.32
450	1.35	1.35	1.35	1.33
500	1.35	1.35	1.35	1.34

1056
 1057

1058 **List of Tables**

1059 1 Review of all the optimization techniques used by the researchers for solving
1060 design optimization problem of RC structures..... 44

1061 2 Beam design details for three different floors - L shaped building frame.....45

1062 3 Typical column design details for all floor - L shaped building frame.....46

1063 4 Beam design details for three different floors- U shaped building frame.....47

1064 5 Typical column design details for all floor –U shaped building frame.....48

1065 6 Monte Carlo Result summary (L shaped frame).....49

1066 7 Monte Carlo Result summary (U shaped frame).....50

1067 8 MATLAB and STAADPro comparison of beam design (L shaped
1068 frame).....51

1069 9 MATLAB and STAADPro comparison of column design (L shaped
1070 frame).....52

1071 10 MATLAB and STAADPro comparison of beam design (U shaped
1072 frame).....53

1073 11 MATLAB and STAADPro comparison of column design (U shaped
1074 frame).....54

1075

1076

1077

Table 1. Review of all the optimization techniques used by the researchers for

1078

solving design optimization problem of RC structures

Authors	Optimization algorithm
Prakash et al.[7]	Simplex and Lagrangian optimization method
Chakrabarty [8]	Geometric programming
Coello et al.[9], Rajeev and Krishnamoorthy[10], Chaudhuri and Maity[20]	Genetic algorithm (GA)
Dole et al. [11]	polynomial optimization technique
De Medeiros et al. [12]	Simulated annealing (SA)
Nigdeli and Bekdaş [13]	random search technique (RST)
Uz et al. [14], Kaveh and Behnam [21]	charged system search (CSS)
Preethi and Arulraj [16]	sequential quadratic programming (SQP)
Bekdaş and Niğdeli [17]	Teaching-learning-based-optimization (TLBO)
Bekdaş and Niğdeli[22]	Harmony search (HS)
Aga and Adam[23]	Artificial neural network (ANN)
Gharehbaghi and Khatibinia[24]	intelligent regression model (IRM) combined with Particle swarm optimization (PSO)
Esfandiary et al. [25, 29]	decision-making Particle Swarm Optimization (DMPSO)
Kulkarni and Bhusare[26]	Response Surface Method (RSM)
Tapao and Cheerarot[28]	Artificial bee colony (ABC)
RazmaraShooli et al. [30]	GA-PSO algorithm
Chaudhuri and Maity [20]	Unified particle swarm optimization (UPSO)

1079

1080

1081

Tables 2 Beam design details for three different floors - L shaped building frame.

Floors	Beam types	Size (mm x mm)	Support (mm)		Mid-span (mm)		Stirrups spacing 8mm ϕ
			Top	Bottom	Top	Bottom	
Top	B1	210x 410	3-12 ϕ	3-12 ϕ	2 -12 ϕ	3-12 ϕ	300
	B2, B3,B4	210x 420	2-16 ϕ	2-12 ϕ	2 -16 ϕ	3-12 ϕ	300
	B5	210x 420	3-12 ϕ	3-12 ϕ	2-12 ϕ	3-12 ϕ	300
6th	B1	210x 390	3- 20 ϕ	2- 20 ϕ	2- 20 ϕ	2- 20 ϕ	300
	B2, B3	270x 530	6-16 ϕ	2- 20 ϕ	2-16 ϕ	2- 20 ϕ	300
	B4	240x 470	4- 20 ϕ	2- 20 ϕ	2- 20 ϕ	3- 20 ϕ	300
	B5	240x 470	5-16 ϕ	2- 20 ϕ	2-16 ϕ	3- 20 ϕ	300
1st	B1	240x 460	5- 20 ϕ	2- 20 ϕ	2- 20 ϕ	3- 20 ϕ	300
	B2	280x 530	6-16 ϕ	2- 20 ϕ	2-16 ϕ	4- 20 ϕ	300
	B3	270x 510	5- 20 ϕ	2- 20 ϕ	2- 20 ϕ	4- 20 ϕ	300
	B4	270x 520	5- 20 ϕ	3- 20 ϕ	2- 20 ϕ	2- 20 ϕ	300
	B5	240x 470	5- 20 ϕ	2- 20 ϕ	2- 20 ϕ	3- 20 ϕ	300

1082

1083

Table 3. Typical Column design details for all floor - L shaped building frame.

Floor s	Column numbers							
	C1		C3		C5		C9	
	Size (mmxmm)	Reinforc ement	Size (mmxmm)	Reinfor cement	Size (mmxmm)	Reinfor cement	Size (mmxmm)	Reinforc ement
8	340x450	12-16 ϕ	320x380	8-16 ϕ	370x280	8-16 ϕ	430x370	8-12 ϕ
7	410x450	12-16 ϕ	330x420	8-20 ϕ	380x330	8-20 ϕ	450x450	8-12 ϕ
6	440x450	12-16 ϕ	350x440	8-20 ϕ	410x370	8-20 ϕ	450x450	8-20 ϕ
5	450x450	12-20 ϕ	370x450	8-20 ϕ	440x410	8-20 ϕ	450x450	8-20 ϕ
4	450x450	12-20 ϕ	410x500	8-20 ϕ	450x430	8-20 ϕ	450x450	8-20 ϕ
3	460x 480	12-20 ϕ	420x500	8-20 ϕ	480x460	8-20 ϕ	470x470	8-20 ϕ
2	500x 500	12-20 ϕ	470x500	8-20 ϕ	490x500	8-20 ϕ	500x500	8-20 ϕ
1	500x 500	12-20 ϕ	500x500	8-20 ϕ	500x500	8-20 ϕ	500x500	8-20 ϕ
G	500x 500	12-20 ϕ	500x500	8-25 ϕ	500x500	8-25 ϕ	500x500	8-25 ϕ

1084

1085

Table 4.Beam design details for three different floors- U shaped building frame

Floors	Beam types	Size (mm x mm)	Support (mm)		Mid-span (mm)		Stirrups spacing 8mm ϕ
			Top	Bottom	Top	Bottom	
Top	B1,B2, B3, B4, B5, B6, B7, B8	200x 380	2-12 ϕ	2-16 ϕ	2 -12 ϕ	2-16 ϕ	300
	B1	220x 430	5- 12 ϕ	2- 16 ϕ	2 -12 ϕ	3-16 ϕ	300
9th	B2, B3	220x 440	5- 12 ϕ	2- 16 ϕ	2 -12 ϕ	3-16 ϕ	300
	B4	230x 450	5- 12 ϕ	2- 16 ϕ	2 -12 ϕ	3-16 ϕ	300
	B5	220x 430	4- 16 ϕ	2- 16 ϕ	2 -16 ϕ	3-16 ϕ	300
	B6, B7	200x 370	4- 16 ϕ	2- 16 ϕ	2 -16 ϕ	2-16 ϕ	300
	B8	220x 350	4- 16 ϕ	2- 16 ϕ	2 -16 ϕ	3-16 ϕ	300
	B1	240x 470	5- 16 ϕ	3-16 ϕ	2 -16 ϕ	4-16 ϕ	300
1st	B2	240x 480	4- 16 ϕ	2- 16 ϕ	2 -16 ϕ	3-16 ϕ	300
	B3	250x 480	4- 16 ϕ	2- 16 ϕ	2 -16 ϕ	4-16 ϕ	300
	B4	230x 450	5- 16 ϕ	3-16 ϕ	2 -16 ϕ	3-16 ϕ	300
	B5	250x 500	4- 16 ϕ	2- 16 ϕ	2 -16 ϕ	4-16 ϕ	300
	B6	240x 430	5- 16 ϕ	3-16 ϕ	2 -16 ϕ	3-16 ϕ	300
	B7	240x 440	5- 16 ϕ	3-16 ϕ	2 -16 ϕ	3-16 ϕ	300
	B8	240x 470	5- 16 ϕ	3-16 ϕ	2 -16 ϕ	3-16 ϕ	300

Table 5. Typical column design details for all floor –U shaped building frame

Floors	Column numbers							
	C1		C3		C5		C9	
	Size (mmxm m)	Reinfor cement	Size (mmxmm)	Reinforc ement	Size (mmxmm)	Reinforc ement	Size (mmxmm)	Reinforc ement
10	330x320	4-12 ϕ	330x260	4-12 ϕ	270 x310	4-12 ϕ	310x310	4-12 ϕ
9	380x350	4-16 ϕ	350x360	4-12 ϕ	330x350	4-16 ϕ	390x320	4-16 ϕ
8	390x370	4-20 ϕ	390x370	4-20 ϕ	350x370	4-20 ϕ	400x380	4-20 ϕ
7	400x390	4-20 ϕ	400x380	4-20 ϕ	360x390	4-20 ϕ	400x390	4-20 ϕ
6	400x400	4-20 ϕ	400x400	4-20 ϕ	380x400	4-20 ϕ	400x400	4-20 ϕ
5	400x400	4-20 ϕ	400x400	4-20 ϕ	390x400	8-20 ϕ	400x400	4-20 ϕ
4	400x400	4-20 ϕ	400x400	4-20 ϕ	390x400	8-20 ϕ	400x400	4-20 ϕ
3	400x400	4-20 ϕ	400x400	4-20 ϕ	390x400	8-20 ϕ	400x400	4-20 ϕ
2	400x400	4-20 ϕ	400x400	8-20 ϕ	400x400	8-20 ϕ	400x400	8-20 ϕ
1	400x400	4-20 ϕ	400x400	8-20 ϕ	400x400	8-20 ϕ	400x400	8-20 ϕ
G	400x400	8-20 ϕ						

1090

Table 6. Monte Carlo Result summary (L shaped framed)

RESULT SUMMARY				
Result after 10 number of experiments				
	Total concrete Rs.	Total formwork Rs.	Total steel Rs.	Total cost Rs.
Mean	1044706.57	883111.02	1928855.23	3856672.82
Standard Deviation (S)	8777.08	4033.53	20228.66	20861.87
Max value	1057596.73	888445.8	1954894.32	3885445.32
Min value	1026706.01	875166.6	1894407.89	3827581.44
MONTE CARLO simulation				
First simulation	1033501.77	875617.80	1934664.40	3885044.13
After 5000 Simulation				
Total cost (Rs.)				
Mean	3856471.18			
Standard Deviation (S)	22264.92			
Min	3792373.03			
Max	3923637.97			
Difference	131264.93			
Increment	6563.24			
Design failure	0			
Key Percentile				
	25%	3841858.21		
	50%	3856822.15		
	75%	3872005.02		
	99%	3926568.36		
Loss percentile	2			

1091

1092

Table 7. Monte Carlo Result summary (U shaped framed)

Result Summary				
Results after 10 number of experiments				
	Total concrete Rs.	Total formwork Rs.	Total steel Rs.	Total cost Rs.
Mean	830104.70	751285.78	1277901.51	2859292.00
Standard Deviation (S)	4042.70	2251.79	6651.91	9282.60
Max value	836727.36	754809.66	1287597.09	2875499.09
Min value	824728.59	747885.6	1270301.75	2847013.56
MONTE CARLO simulation				
First simulation	820513.55	754301.59	1272679.41	2863711.65
After 5000 Simulation				
Total cost (Rs.)				
Mean	2859591.13			
Standard Deviation (S)	7680.10			
Min	2833889.28			
Max	2887321.15			
Difference	53431.86			
Increment	2671.59			
Design failure	0			
Key Percentile				
	25%	2853784.32		
	50%	2859260.04		
	75%	2864541.17		
	99%	2881806.97		
Loss percentile	0.6			

1096

Table 8.Comparison of beam design forces before and after optimization(L shaped frame)

Fourth floor	Beam No.	Size (mm x mm)	Bending moment (kN-m)			Shear force (KN)
			Support top	Support bottom	Midspan bottom	
Before	B1	270 x 530	249	117	51	155
After			233	111	50	144
Before	B2	280 x 490	255	130	50	150
After			242	122	60	144
Before	B3	240 x 400	260	133	61	152
After			243	125	60	144
Before	B4	240 x 440	263	137	61	153
After			260	143	64	144
Before	B5	220 x 430	260	131	60	153
After			260	130	54	144

1097

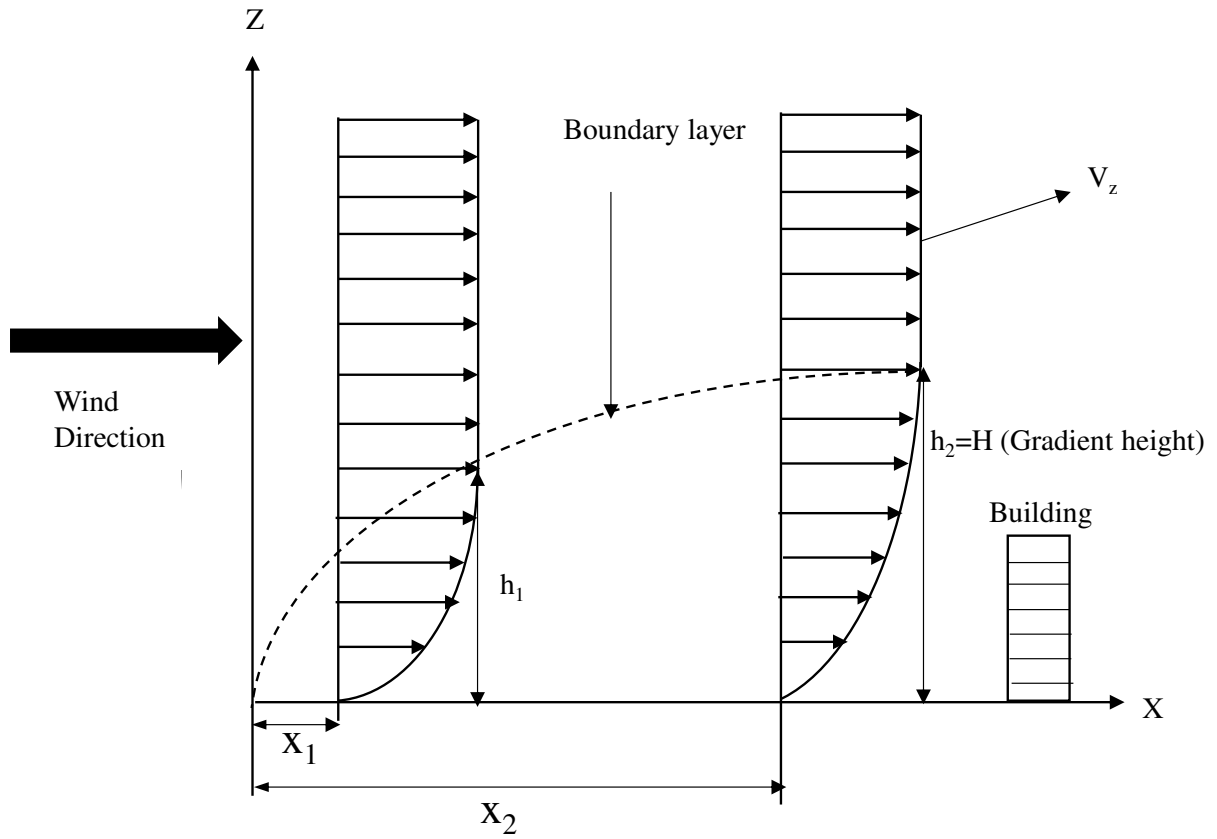
1098

Table 9. Comparison of column design forces before and after optimization(L shaped frame)

Fourth floor	Column No.	Size (mm x mm)	Axial force (kN)	Bending moment (kN-m)	
				M _z	M _y
Before	C1	450 x 450	1587	254	9
After			1575	207	3
Before	C2	450 x 450	1262	250	37
After			1231	216	35
Before	C3	450 x 450	1125	41	184
After			1096	39	173
Before	C4	420 x 450	1537	6	232
After			1505	4	205
Before	C5	450 x 450	1565	1.49	250
After			1507	1.3	224
Before	C6	430 x 450	1217	40	227
After			1210	37	219
Before	C7	450 x 450	1523	221	6
After			1508	204	3.6
Before	C8	400 x 400	1262	181	40
After			1247	175	38
Before	C9	450 x 390	1245	184	41
After			1230	178	39
Before	C10	450 x 430	1123	148	39
After			1106	144	38
Before	C11	450 x 400	1246	230	43
After			1186	227	41
Before	C12	450 x 450	1110	220	43
After			997	199	40

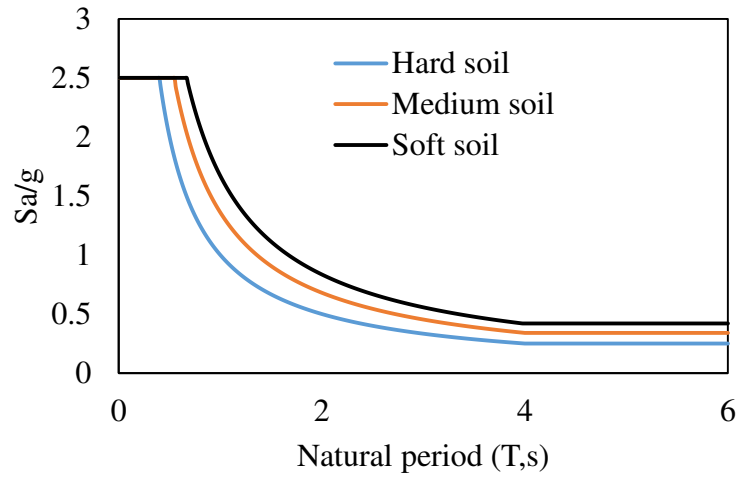
1102 **List of Figures**

1103 1 Typical velocity profile of wind moving through a particular terrain (x_1 , x_2 =fetch
1104 length; h_1 , h_2 =developed height).....54
1105 2 Design acceleration response spectrum of IS 1893-2016(Part-III) [43].....55
1106 3 a) Typical reinforcement detail of column section b) Strain diagram of concrete
1107 section when neutral axis lies inside the section c) Strain diagram of concrete
1108 section when neutral axis lies outside the section d) Stress diagram of concrete
1109 section when neutral axis lies outside the
1110 section.....56
1111 4 Flowchart for cost optimization of whole frame.....57
1112 5 Formwork profile of member cross sections: a) beam b) column.....58
1113 6 Typical floor grid plan of the building frames showing beams and column
1114 positions a) L shaped building b) U shaped
1115 building.....59
1116 7 Wind profile used wind load analysis a) Velocity profile b) Pressure profile....60
1117 8 Schematic diagram of continuous beam showing the details of curtailments in
1118 bars.....61
1119 9 Design optimization results for L-shaped building frame. (a)convergence curve of
1120 total cost for different grade concrete along with Fe 415 steel.(b)convergence
1121 curve for cost of different parameters for M20 concrete and Fe 415 steel. (c)
1122 Variation of total cost for different concrete and steel grades62
1123 10 Design optimization results for U-shaped building frame. (a)convergence curve of
1124 total cost for different grade concrete along with Fe 415 steel.(b)convergence
1125 curve for cost of different parameters for M25 concrete and Fe 415 steel. (c)
1126 Variation of total cost for different concrete and steel grades63
1127 11 Probability distribution for 5000 simulated solutions (L shaped
1128 frame).....64
1129 12 Probability distribution for 5000 simulated solutions (U shaped
1130 frame).....65
1131



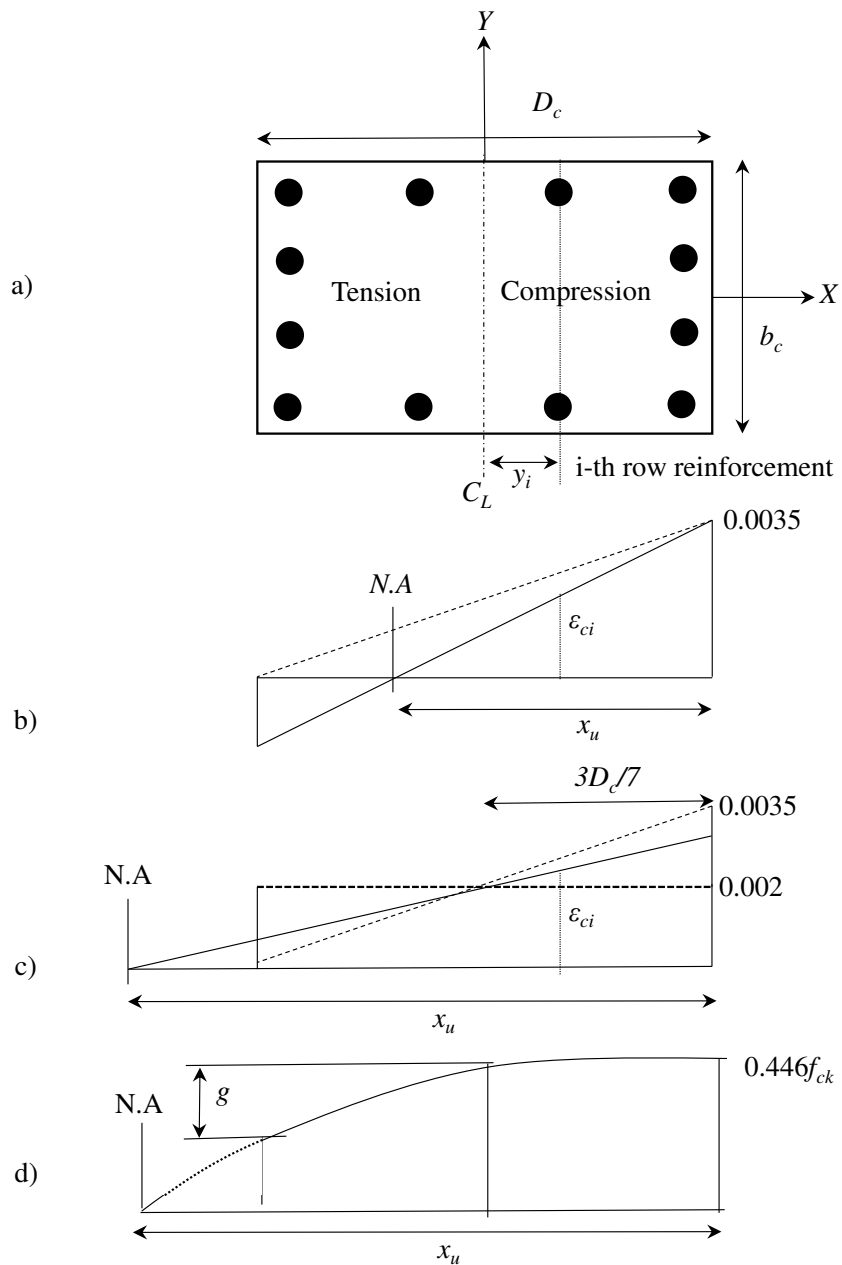
1132
 1133
 1134
 1135
 1136
 1137
 1138
 1139
 1140

Fig.1. Typical velocity profile of wind moving through a particular terrain (x_1, x_2 =fetch length; h_1, h_2 =developed height)



1141
 1142
 1143
 1144
 1145
 1146
 1147

Fig.2.Design acceleration response spectrum of IS 1893-2016(Part-III)[43]



1149

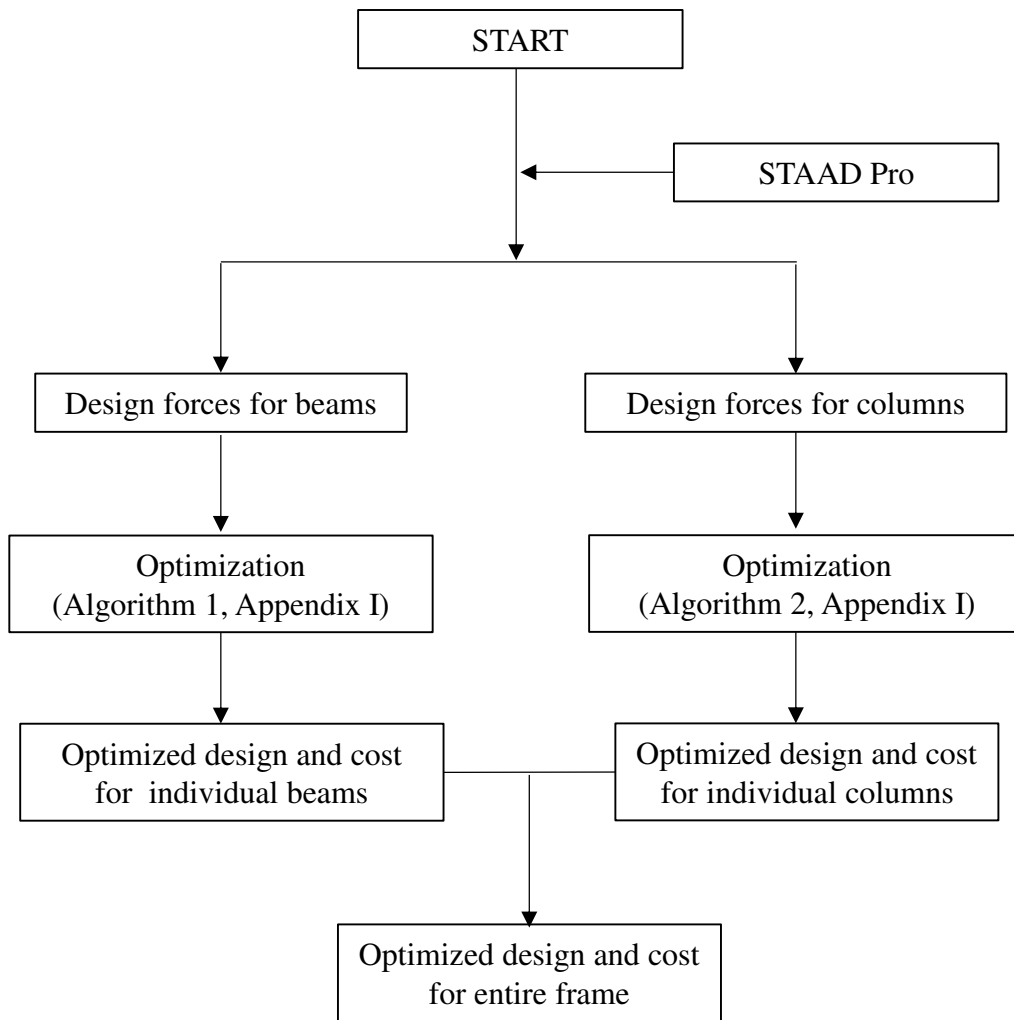
1150 **Fig. 3.**a) Typical reinforcement detail of column section b) Strain diagram of concrete section

1151 when neutral axis lies inside the section c) Strain diagram of concrete section when neutral

1152 axis lies outside the section d) Stress diagram of concrete section when neutral axis lies

1153 outside the section

1154



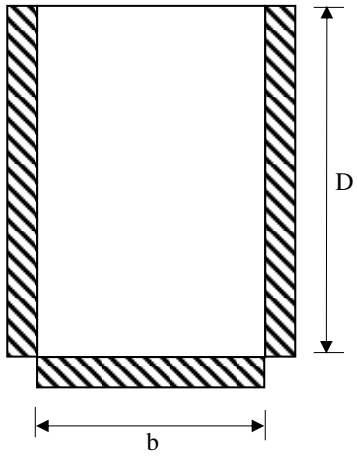
1155

1156

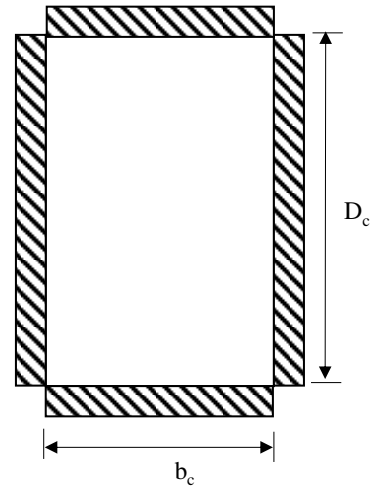
Fig.4. Flowchart for cost optimization of whole frame

1157

a)



b)



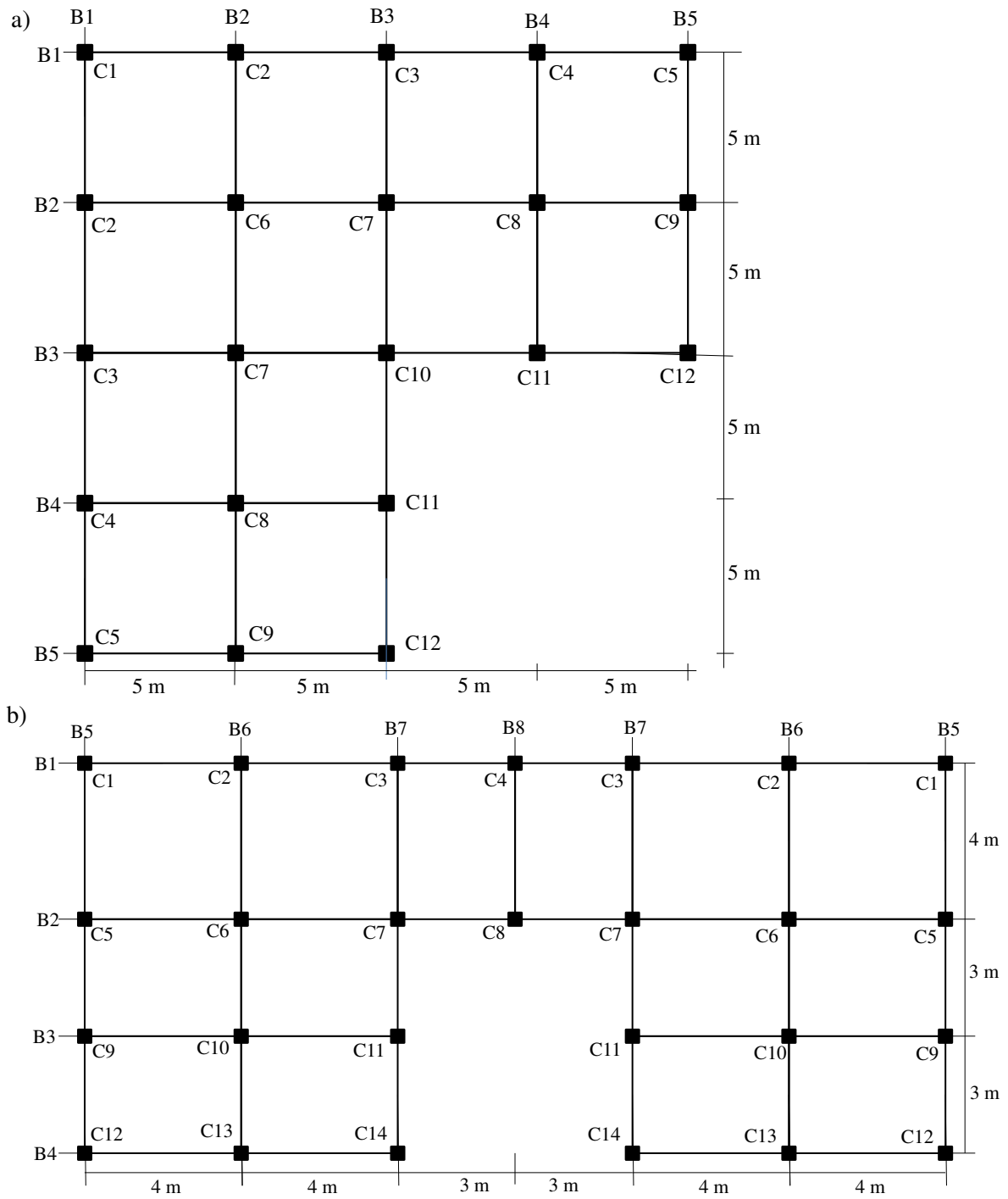
1158

1159

1160

Fig.5.Formwork profile for member cross section: a) Beam b) Column

1161



1162

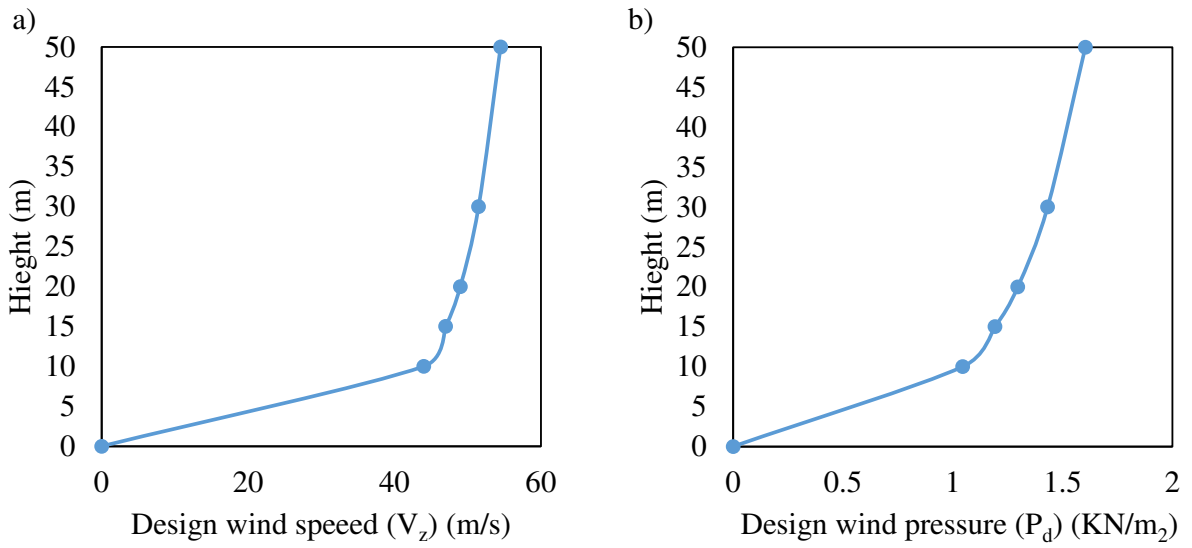
1163 **Fig. 6.** Typical floor grid plan of the building frames showing beams and column positions a)

1164

L shaped building b) U shaped building

1165

1166



1167

1168

1169

1170

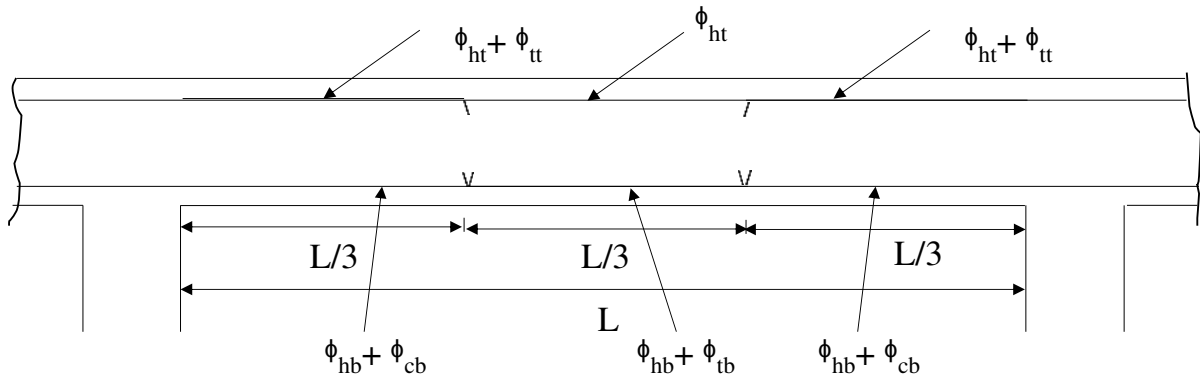
Fig. 7. Wind profile used wind load analysis a) Velocity profile b) Pressure profile

1171

1172

1173

1174



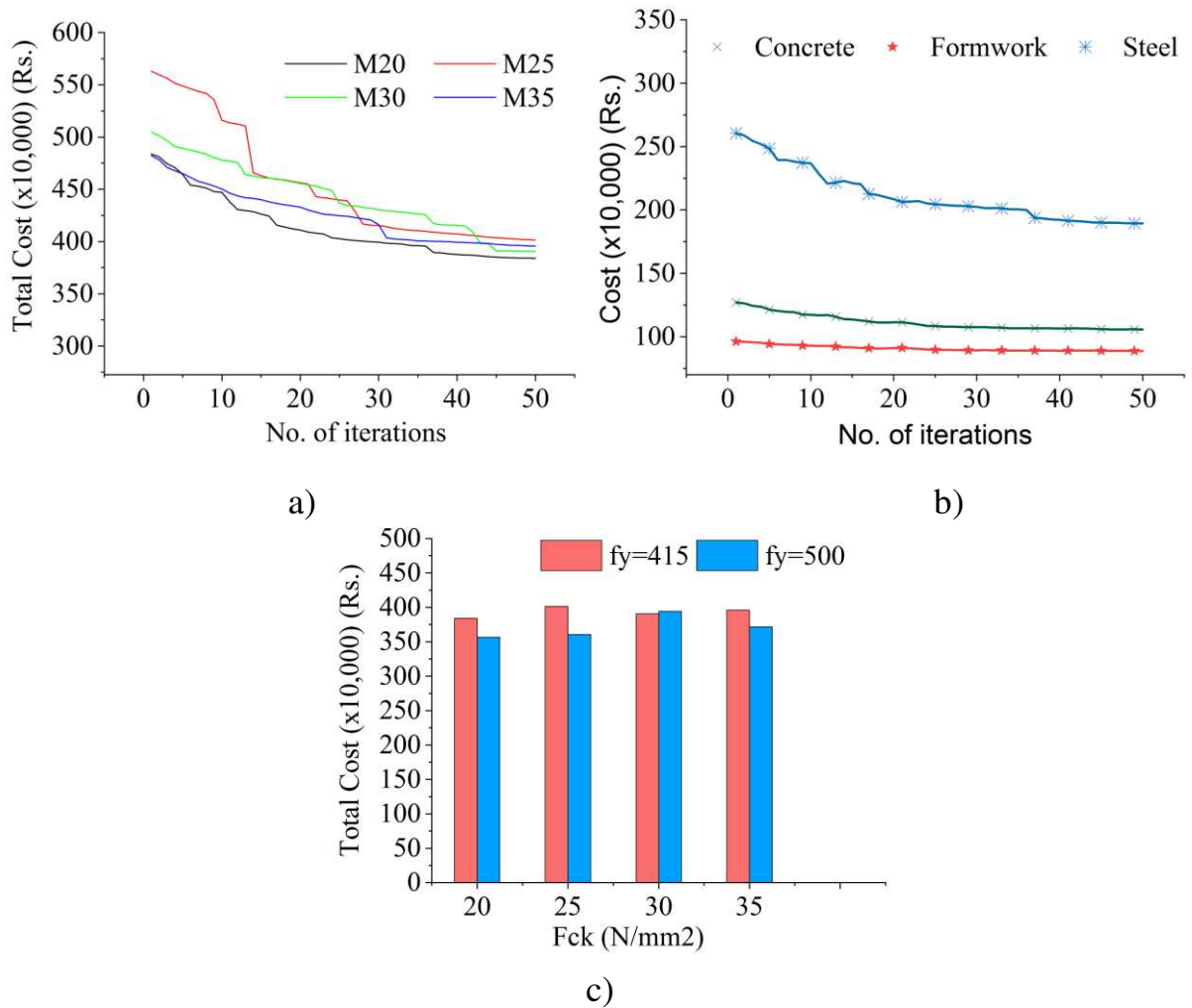
ϕ_{ht} = hanger bars at top, ϕ_{tt} = extra bars at support top due to tension, ϕ_{hb} = hanger bars at bottom, ϕ_{cb} = extra bars at support bottom due to compression, ϕ_{tb} = extra bars at mid-span bottom due to tension

1175

1176

1177 **Fig. 8.** Schematic diagram of continuous beam showing the details of curtailments in bars

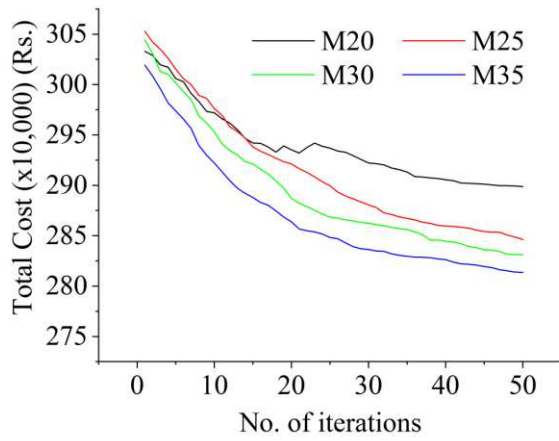
1178



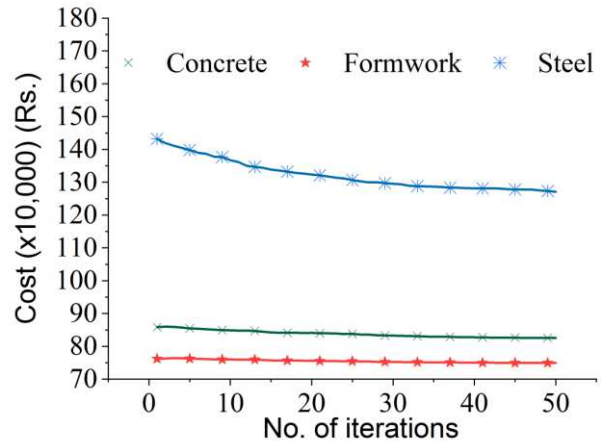
1179

1180 **Fig. 9.** Design optimization results for L-shaped building frame. (a) convergence curve of
 1181 total cost for different grade concrete along with Fe 415 steel.(b) convergence curve for cost
 1182 of different parameters for M20 concrete and Fe 415 steel. (c) Variation of total cost for
 1183 different concrete and steel grades

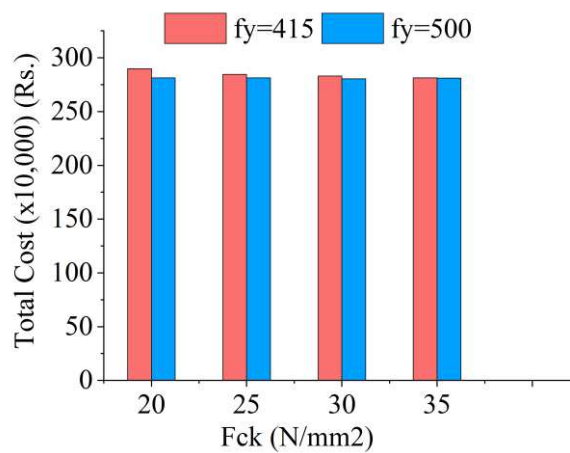
1184



a)



b)

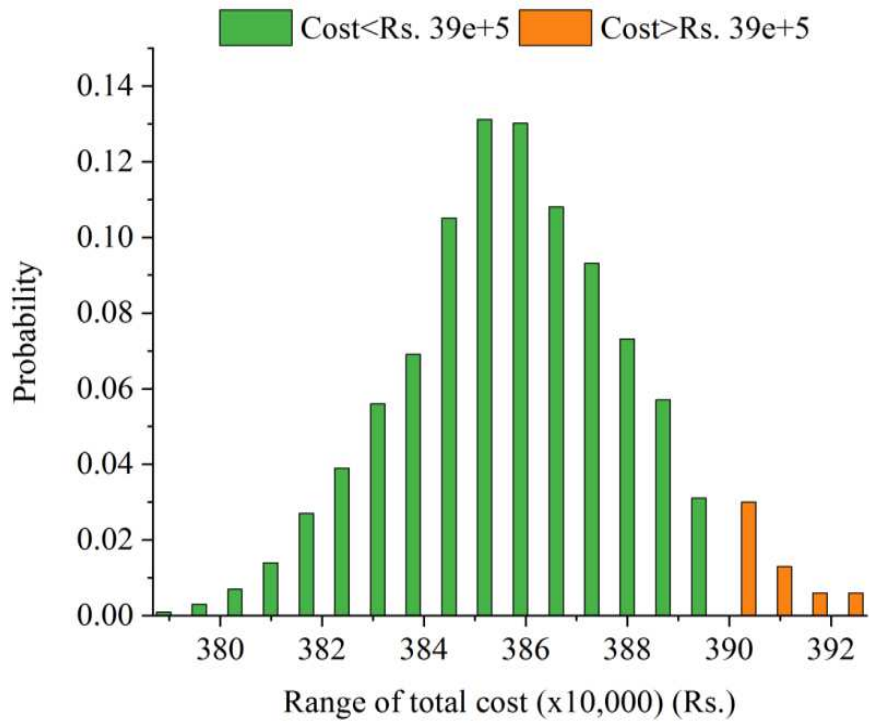


c)

1185

1186 **Fig. 10.** Design optimization results for U-shaped building frame. (a) convergence curve of
 1187 total cost for different grade concrete along with Fe 415 steel. (b) convergence curve for cost
 1188 of different parameters for M25 concrete and Fe 415 steel. (c) Variation of total cost for
 1189 different concrete and steel grades

1190

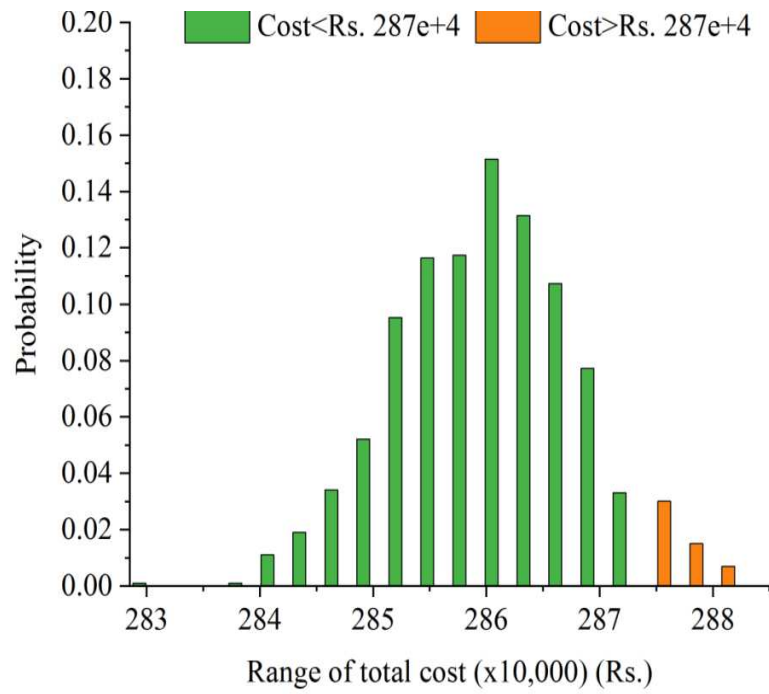


1191

1192

Fig.11. Probability distribution for 5000 simulated solutions (L shaped frame)

1193



1194

1195 **Fig. 12.**Probability distribution for 5000 simulated solutions (U shaped frame)

1196

Figures

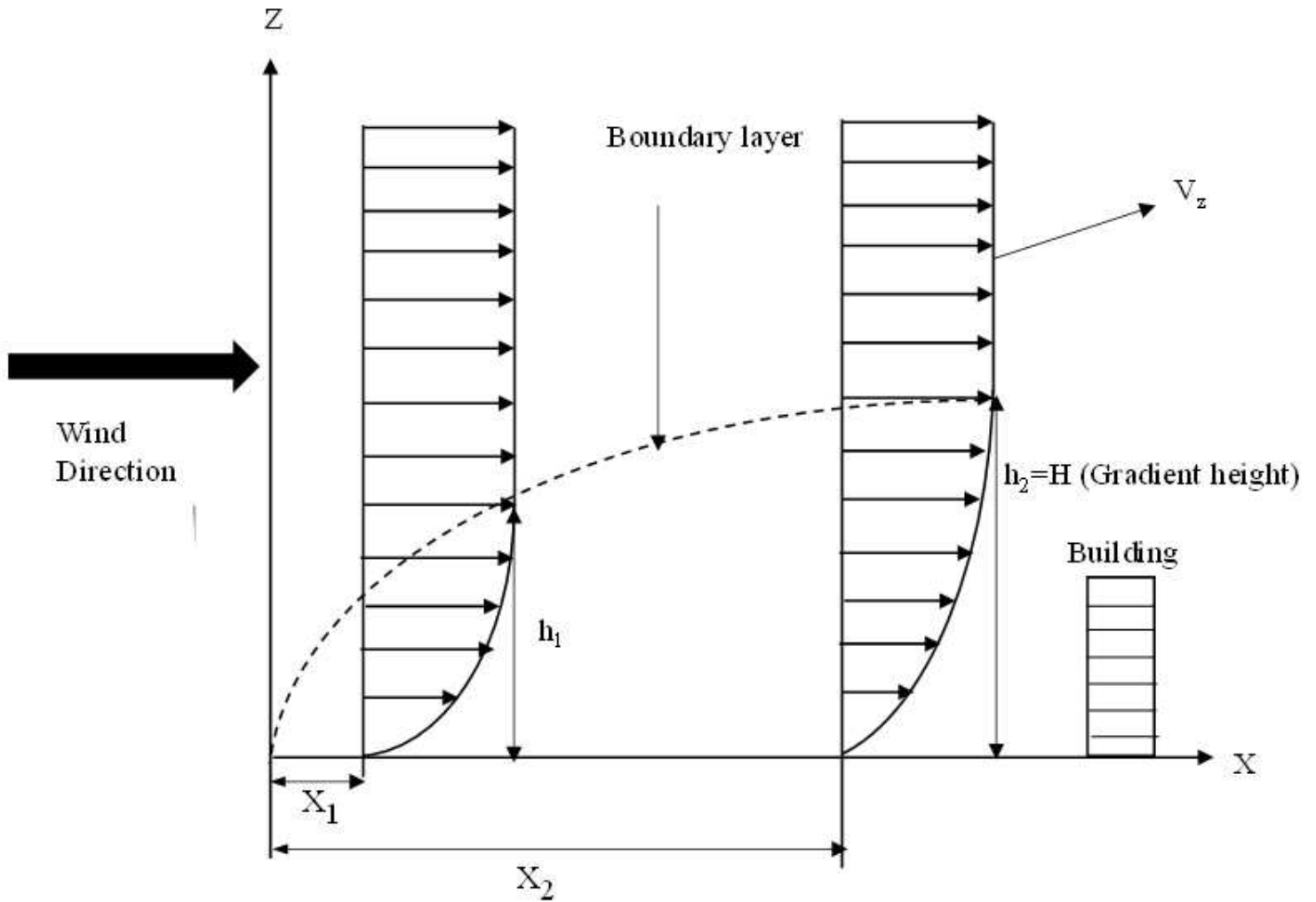


Figure 1

Typical velocity profile of wind moving through a particular terrain (x_1, x_2 =fetch length; h_1, h_2 =developed height)

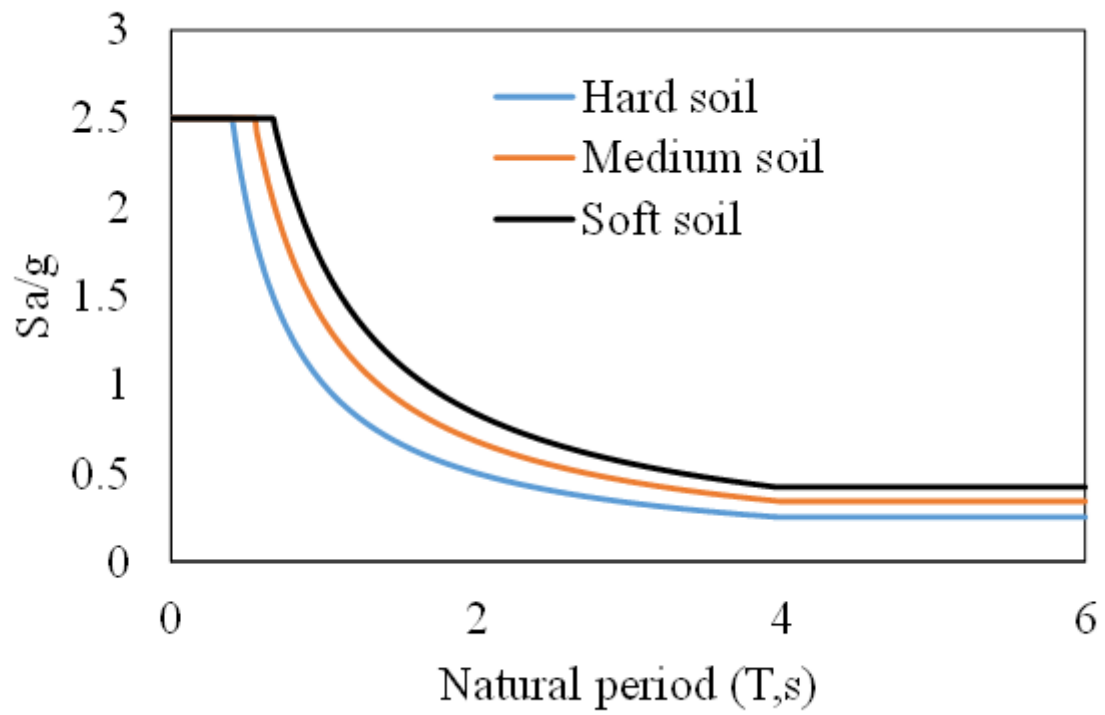


Figure 2

Design acceleration response spectrum of IS 1893-2016(Part-III)[43]

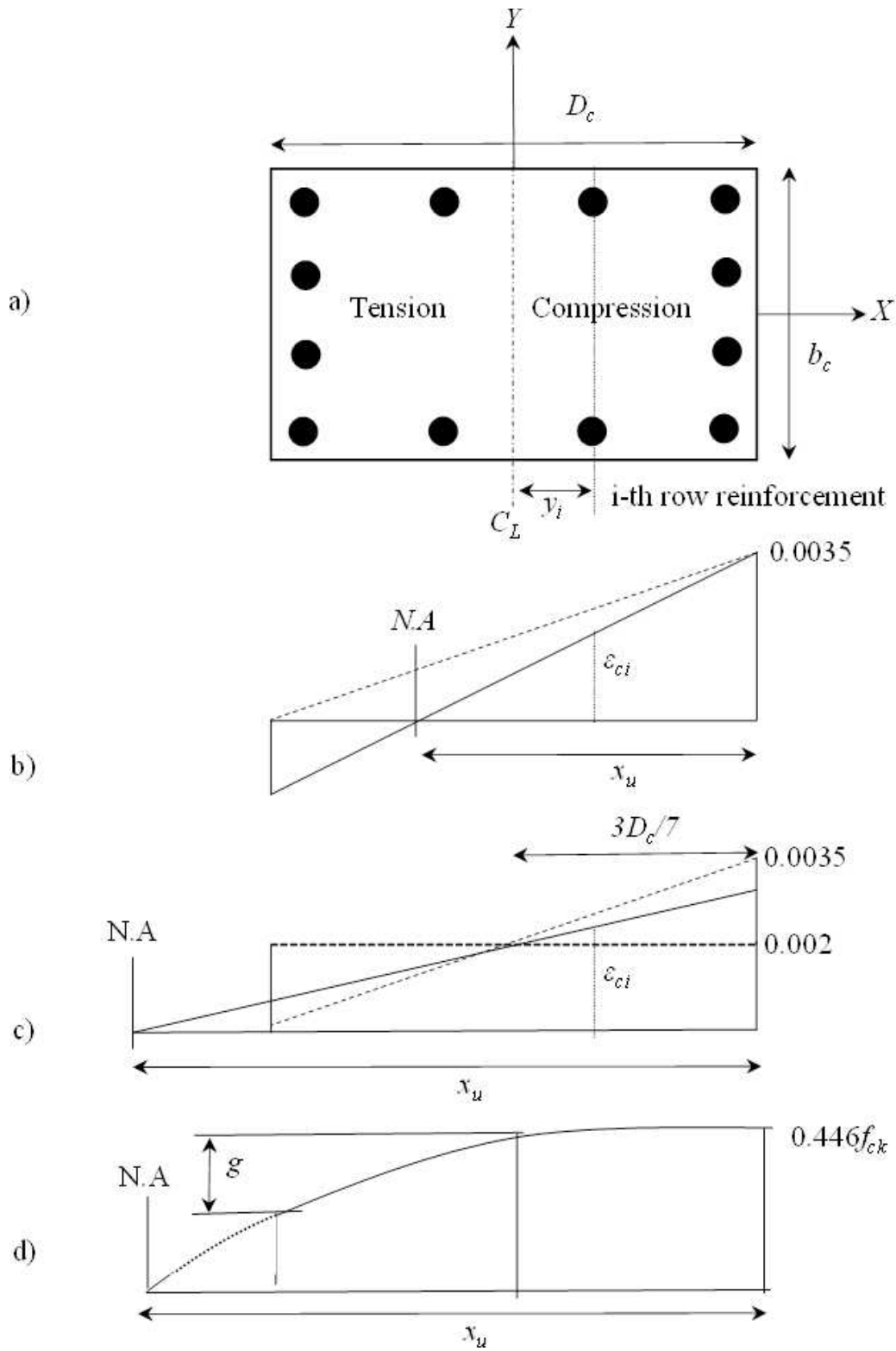


Figure 3

a) Typical reinforcement detail of column section b) Strain diagram of concrete section when neutral axis lies inside the section c) Strain diagram of concrete section when neutral axis lies outside the section d) Stress diagram of concrete section when neutral axis lies outside the section

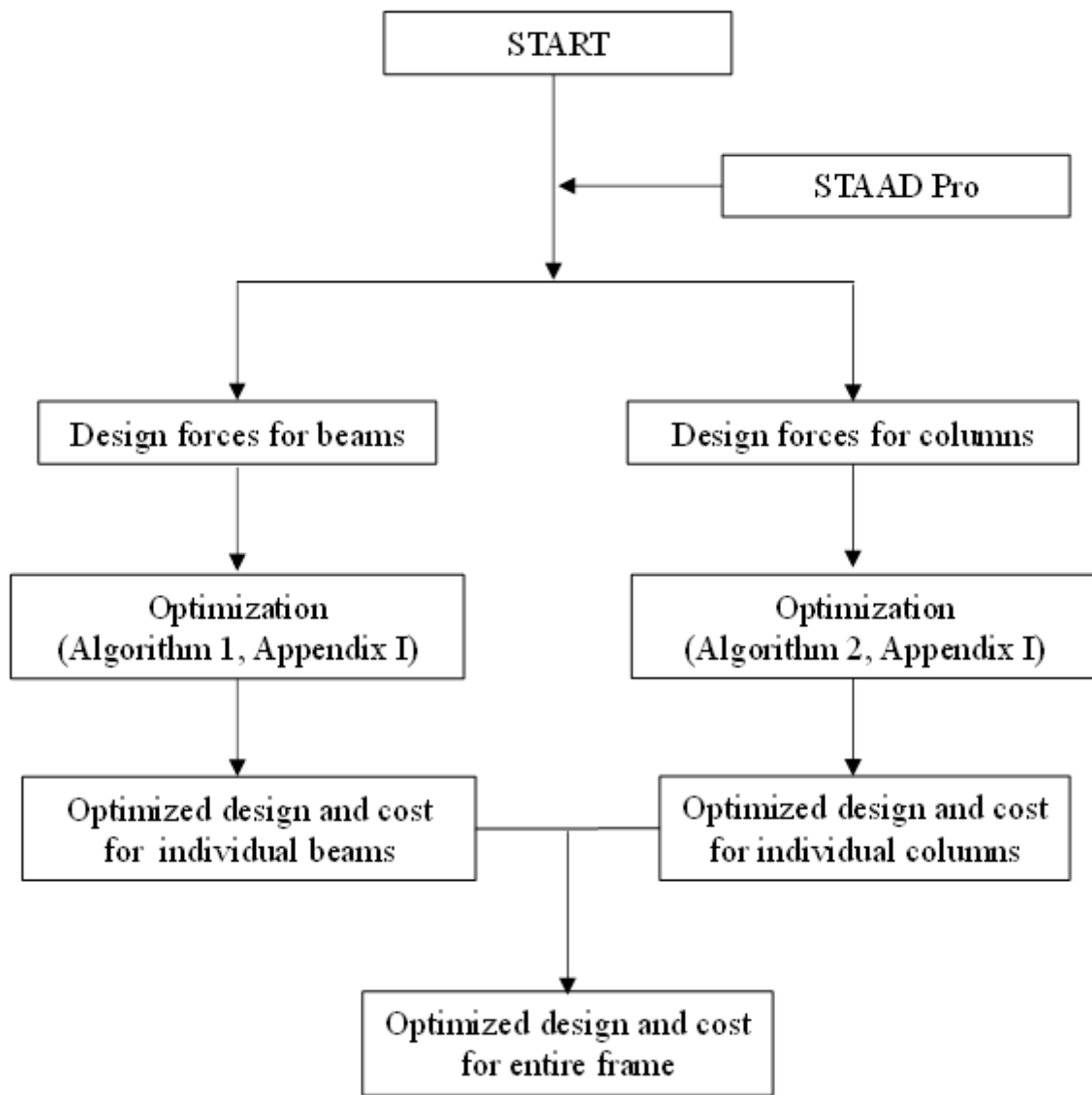


Figure 4

Flowchart for cost optimization of whole frame

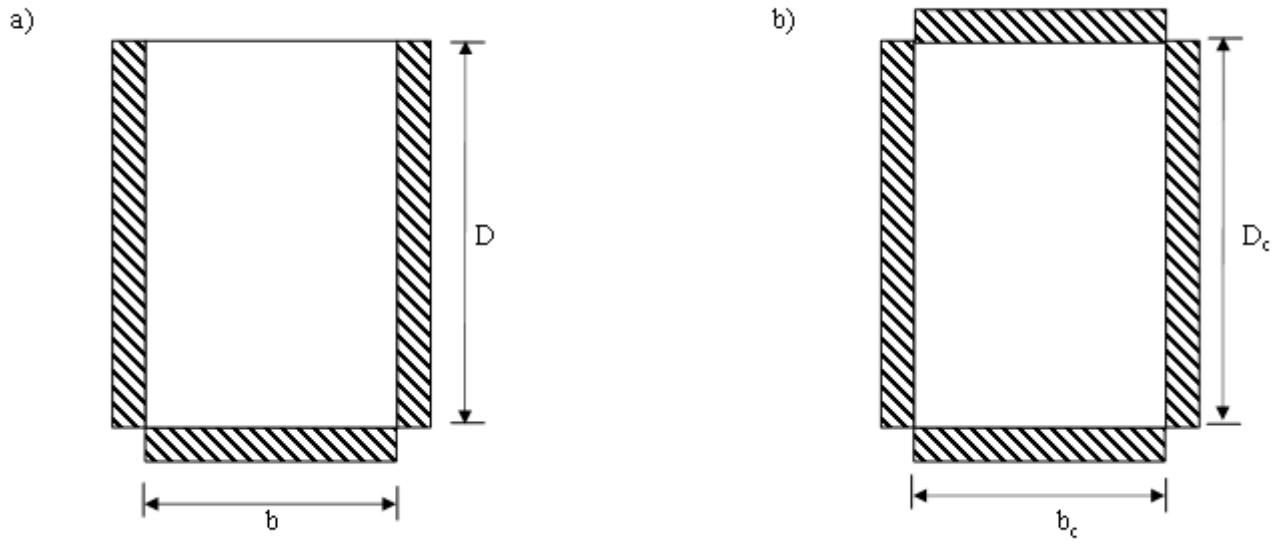


Figure 5

Formwork profile for member cross section: a) Beam b) Column

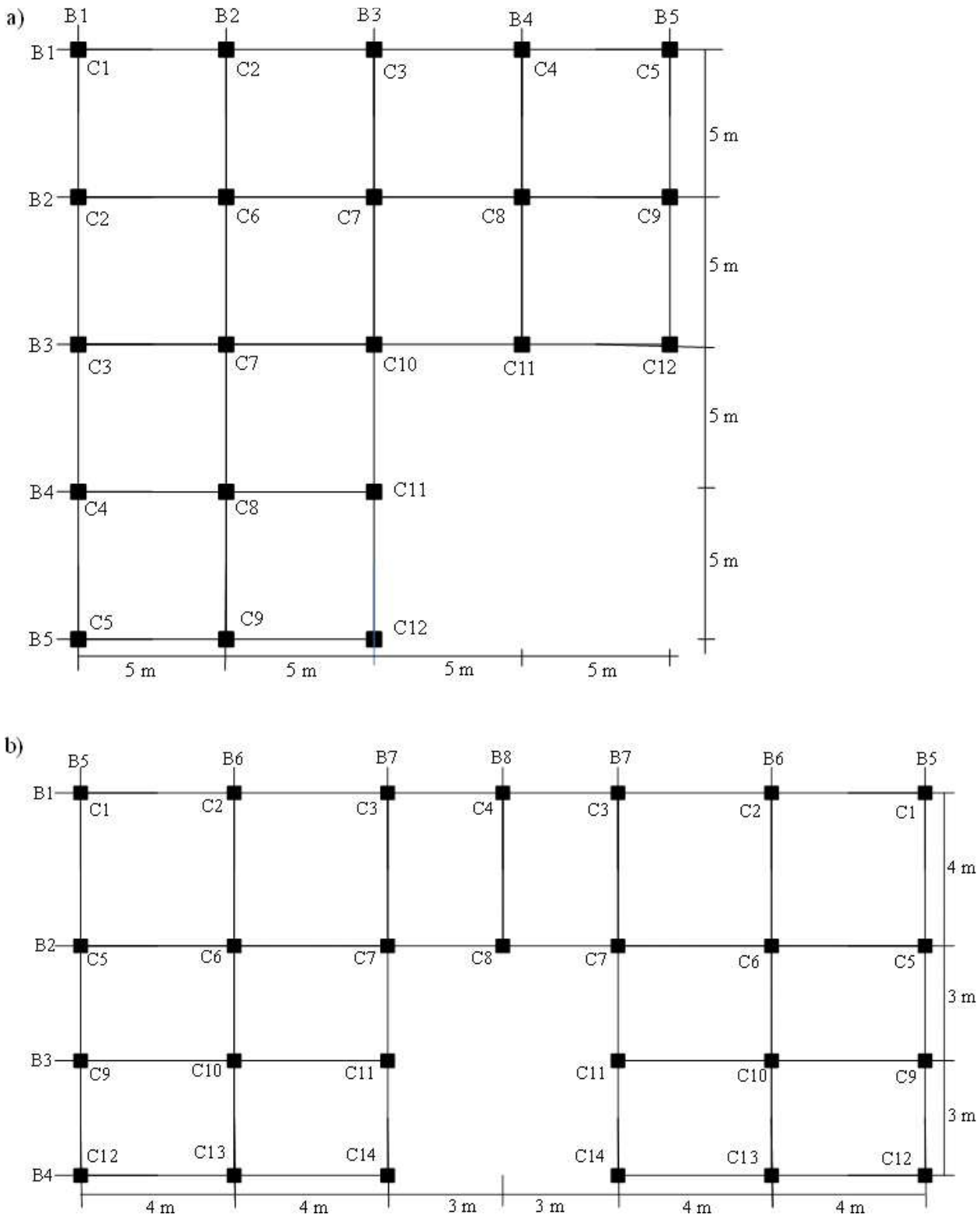


Figure 6

Typical floor grid plan of the building frames showing beams and column positions a) L shaped building
 b) U shaped building

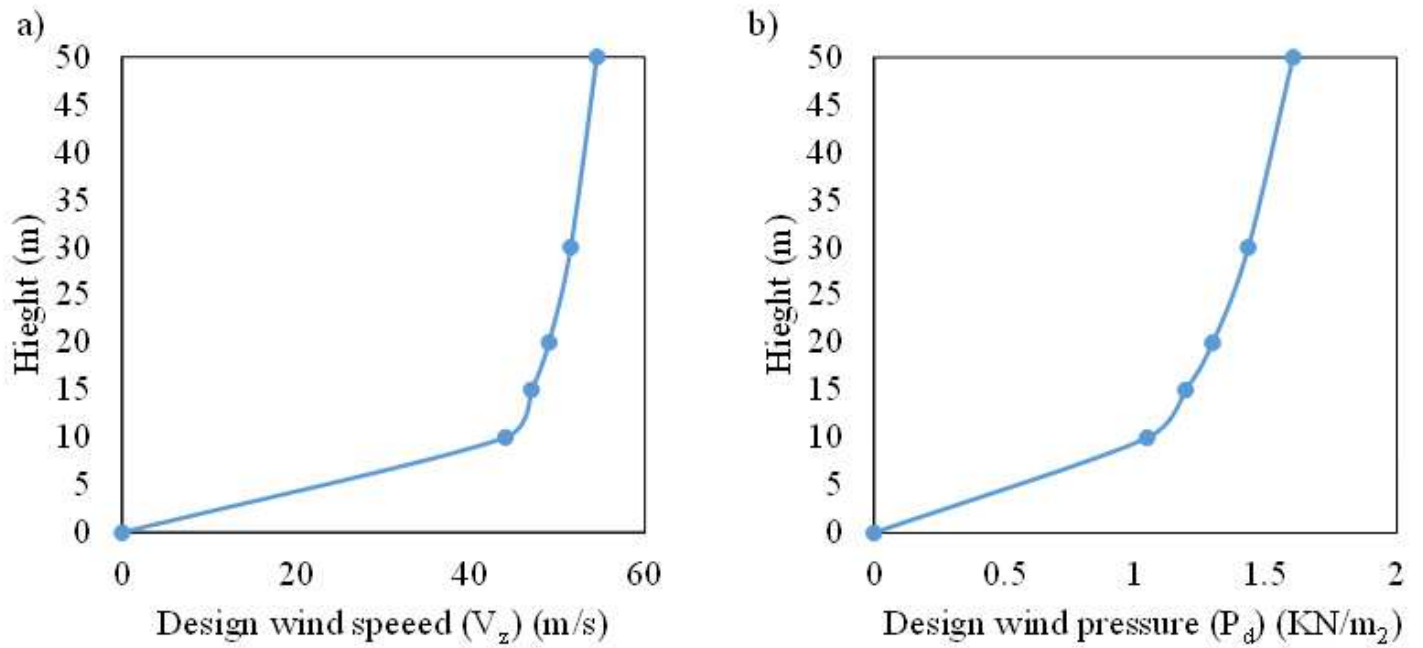
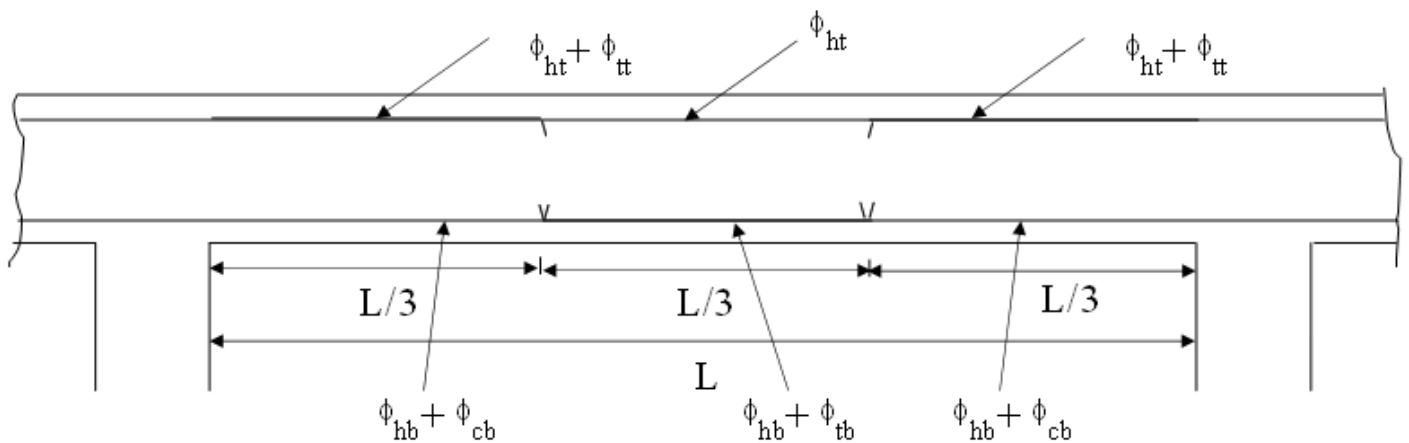


Figure 7

Wind profile used wind load analysis a) Velocity profile b) Pressure profile



ϕ_{ht} = hanger bars at top, ϕ_{tt} = extra bars at support top due to tension, ϕ_{hb} = hanger bars at bottom, ϕ_{cb} = extra bars at support bottom due to compression, ϕ_{tb} = extra bars at mid-span bottom due to tension

Figure 8

Schematic diagram of continuous beam showing the details of curtailments in bars

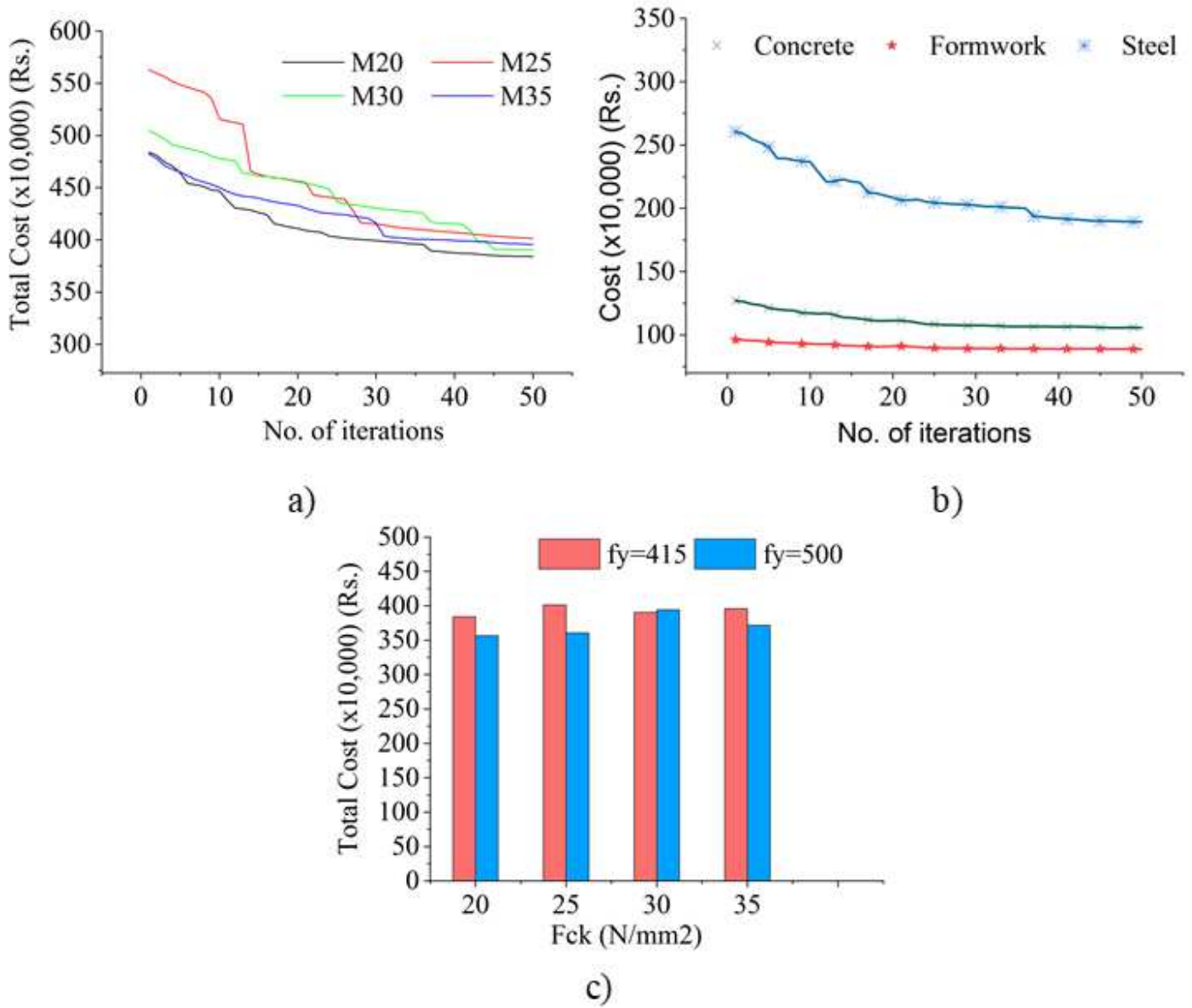
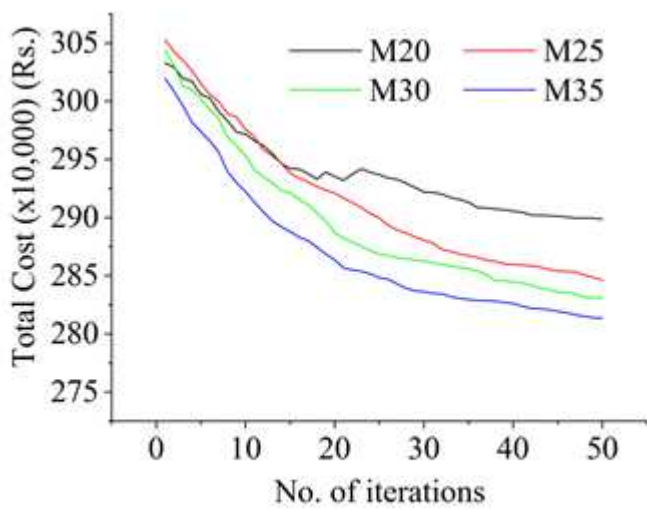
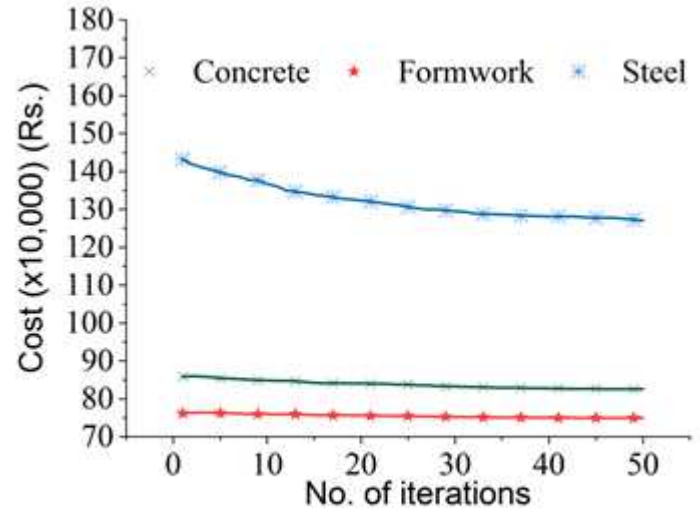


Figure 9

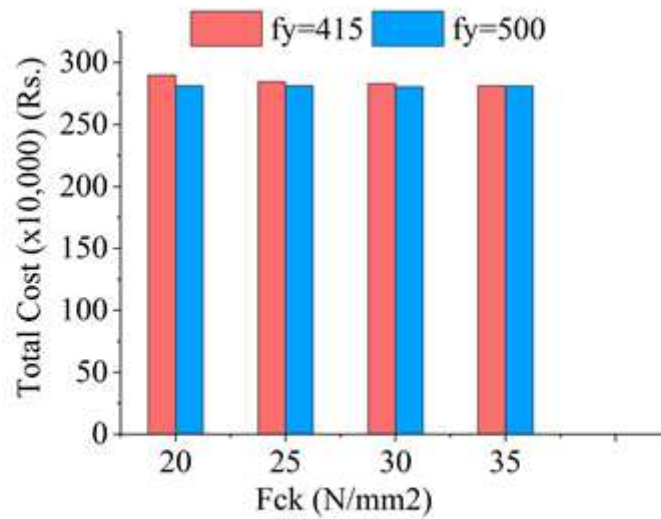
Design optimization results for L-shaped building frame. (a) convergence curve of total cost for different grade concrete along with Fe 415 steel. (b) convergence curve for cost of different parameters for M20 concrete and Fe 415 steel. (c) Variation of total cost for different concrete and steel grades



a)



b)



c)

Figure 10

Design optimization results for U-shaped building frame. (a) convergence curve of total cost for different grade concrete along with Fe 415 steel. (b) convergence curve for cost of different parameters for M25 concrete and Fe 415 steel. (c) Variation of total cost for different concrete and steel grades

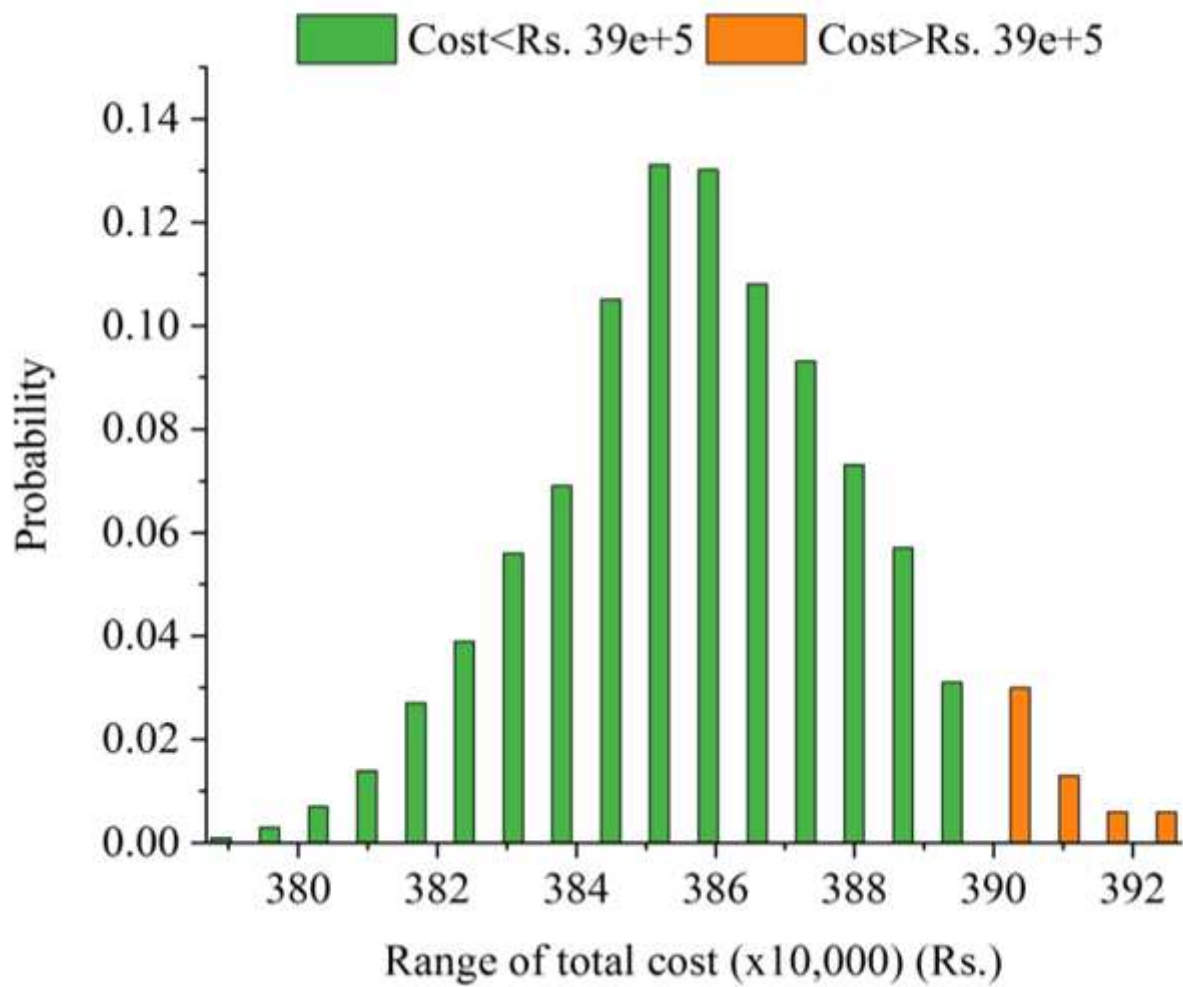


Figure 11

Probability distribution for 5000 simulated solutions (L shaped frame)

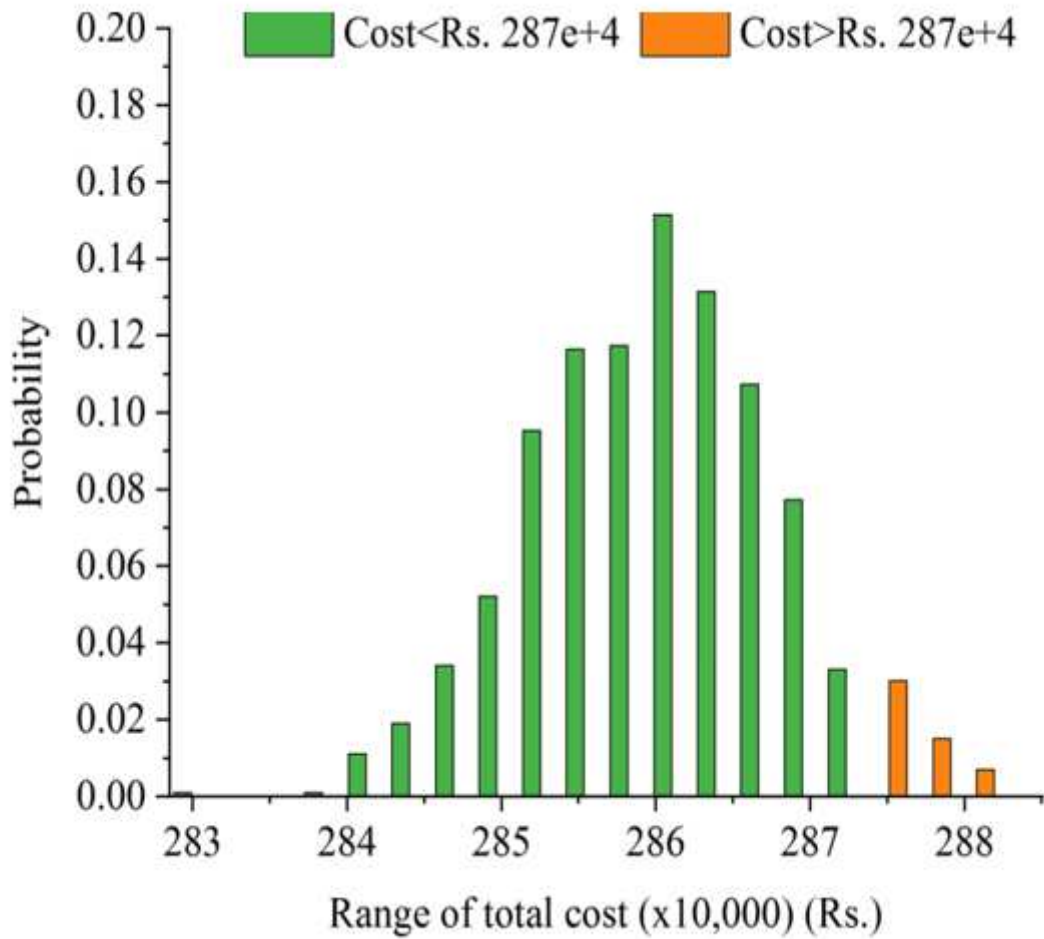


Figure 12

Probability distribution for 5000 simulated solutions (U shaped frame)

Supplementary Files

This is a list of supplementary files associated with this preprint. Click to download.

- [APPENDIX.docx](#)